

## Calibration of excess thermodynamic properties and elastic constant variations associated with the $\alpha \leftrightarrow \beta$ phase transition in quartz

MICHAEL A. CARPENTER,<sup>1</sup> EKHARD K.H. SALJE,<sup>1</sup> ANN GRAEME-BARBER,<sup>1</sup>  
BERND WRUCK,<sup>1</sup> MARTIN T. DOVE,<sup>1</sup> AND KEVIN S. KNIGHT<sup>2</sup>

<sup>1</sup>Department of Earth Sciences, University of Cambridge, Downing Street, Cambridge CB2 3EQ, U.K.

<sup>2</sup>ISIS Facility, Rutherford Appleton Laboratory, Chilton, Didcot, Oxfordshire, OX11 0QX, U.K.

### ABSTRACT

Spontaneous strains for the  $\alpha \leftrightarrow \beta$  transition in quartz were determined from lattice parameter data collected by X-ray powder diffraction and neutron powder diffraction over the temperature range  $\sim 5$ –1340 K. These appear to be compatible with previous determinations of the order parameter variation in  $\alpha$  quartz only if there is a non-linear relationship between the individual strains and the square of the order parameter. An expanded form of the 2-4-6 Landau potential usually used to describe the phase transition was developed to account for these strains and to permit calculation of the elastic constant variations. Calibration of the renormalized coefficients of the basic 2-4-6 potential, using published heat capacity data, provides a quantitative description of the excess free energy, enthalpy, entropy, and heat capacity. Values of the unrenormalized coefficients in the Landau expansion that include all the strain-order parameter coupling coefficients were used to calculate variations of the elastic constants. Values of the bare elastic constants were extracted from published elasticity data for  $\beta$  quartz. Calculated variations of  $C_{11}$  and  $C_{12}$  match their observed variations closely, implying that the extended Landau expansion provides a good representation of macroscopic changes within the (001) plane of quartz. Agreement was not as close for  $C_{33}$ , suggesting that other factors may influence the strain parallel to [001]. The geometrical mechanism for the transition involves both rotations and shearing of  $\text{SiO}_4$  tetrahedra, with each coupled differently to the driving order parameter. Only the shearing part of the macroscopic distortions appears to show the same temperature dependence as other properties that scale with  $Q^2$ . Coupling between the strain and the order parameter provides the predominant stabilization energy for  $\alpha$  quartz and is also responsible for the first-order character of the transition.

### INTRODUCTION

Because of its geological and technological importance, quartz has attracted the attention of scientists in diverse fields. Of particular interest have been the marked changes in physical and thermodynamic properties that accompany the  $\alpha \leftrightarrow \beta$  transition. Relationships between these properties are generally described using two different approaches. Several authors have used the Pippard equations for a  $\lambda$  transition (Pippard 1956; Garland 1964) to relate heat capacity, thermal expansion, and elastic compliances (e.g., Hughes and Lawson 1962; Garland 1964; Klement and Cohen 1968; Coe and Paterson 1969; Bachheimer and Dolino 1980; Dolino et al. 1983; Hosieni et al. 1985; Dorogokupets 1995). Others have used standard Landau free energy expansions (Höchli and Scott 1971; Grimm and Dorner 1975; Bachheimer and Dolino 1975; Banda et al. 1975; Dolino and Bachheimer 1982; Dolino et al. 1983; Salje et al. 1992). Landau theory may be expected to fail in the close vicinity of a critical point but should provide a valid description of the behavior over many hundreds of degrees away from the transition

point. On the other hand, the Pippard equations were designed to characterize thermodynamic properties as a transition point is approached and do not necessarily represent the behavior over the wider temperature interval (see discussion in Klement and Cohen 1968). Given the amount of work that has been done on quartz, it is somewhat surprising that a comprehensive description of the relationships among elastic constants, spontaneous strain, and excess energy has not been published. Data for the elastic constants have been available since the 1940s (Atanasoff and Hart 1941; Atanasoff and Kammer 1948; Kammer et al. 1948), and numerous studies of thermal expansion appear in the literature (summarized in Ackermann and Sorrell 1974; Bachheimer and Dolino 1975; Ghiorso et al. 1979; Dolino and Bachheimer 1982). The formal dependence of these properties on the driving order parameter is also known (e.g., Höchli and Scott 1971; Bachheimer and Dolino 1975), but values for the relevant coupling coefficients have not been determined. The primary objective of the present paper is to fill this apparent gap. High-temperature lattice parameters were redeter-

mined for this purpose, and values for all the required coefficients in a full Landau expansion have been derived. The elastic constant variations were then calculated, leading to some reanalysis of both the microscopic and macroscopic mechanisms of the phase transition.

The most characteristic features of the  $\alpha \leftrightarrow \beta$  quartz transition have been discussed by Dolino (1988, 1990) and Dolino et al. (1992), and more recent reviews of the literature are included in Heaney (1994), Dolino and Valade (1994), and Dorogokupets (1995). A summary of earlier thermodynamic data was given by Ghiorso et al. (1979). The incommensurate phase is stable only over a temperature interval of less than 2 K above the transition point and probably does not have a direct bearing on the thermodynamic behavior over the much wider temperature interval considered here.

This paper is divided into eight main sections. The bare essentials of Landau theory required to describe the transition are set out first. In the second section, spontaneous strain data are extracted from high-temperature lattice parameter measurements. New sets of X-ray and neutron diffraction data were collected because the central issue is the relationship between strain and the driving order parameter,  $Q$ . Next, published data for the heat capacity,  $C_p$ , are used to determine absolute values for the coefficients of terms in  $Q$  alone. In the fourth section, elastic constant data for temperatures above the transition point are fit with a standard expression to obtain values for the bare elastic constants of  $\beta$  quartz (i.e., excluding the influence of the transition). To test the model, values of the elastic constants calculated by using the Landau expansion for temperatures below the transition point are compared with measured values from the literature. The final three sections deal with insights that the numerical results provide into the relative importance of the soft mode and elastic energies in stabilizing  $\alpha$  quartz, the relationship between microscopic distortions of the structure and macroscopic strain, and consideration of whether the transition can be treated as an elastic instability.

### LANDAU THEORY

It is well established that the macroscopic evolution of quartz at and below the  $\alpha \leftrightarrow \beta$  transition point can be described by the standard Landau expansion for a first-order transition (Grimm and Dorner 1975; Bachheimer and Dolino 1975; Banda et al. 1975; Dolino and Bachheimer 1982). Odd order terms in  $Q$  are not permitted by symmetry and the expansion is written as:

$$G = \frac{1}{2}a(T - T_c)Q^2 + \frac{1}{4}b^*Q^4 + \frac{1}{6}c^*Q^6 \quad (1)$$

where  $b^*$  and  $c^*$  are the renormalized fourth and sixth order coefficients (including the effects of strain-order parameter coupling). If  $b^*$  is negative, the equilibrium evolution of  $Q$  is given by:

$$Q^2 = \frac{2}{3}Q_0^2 \left\{ 1 + \left[ 1 - \frac{3}{4} \left( \frac{T - T_c}{T_{tr} - T_c} \right) \right]^{1/2} \right\}. \quad (2)$$

At the equilibrium transition temperature,  $T_{tr}$ , there is a jump in the value of  $Q$  from zero to  $Q_0$ , where:

$$Q_0^2 = -\frac{4a}{b^*}(T_{tr} - T_c). \quad (3)$$

The difference between  $T_{tr}$  and  $T_c$  may also be expressed as:

$$(T_{tr} - T_c) = \frac{3(b^*)^2}{16ac^*} \quad (4)$$

and is a measure of how close the first-order transition is to being tricritical in character ( $b^* < 0$  and  $T_{tr} > T_c$  for first order,  $b^* = 0$  and  $T_{tr} = T_c$  for tricritical character).

The excess enthalpy and entropy associated with the transition are given in the usual way by:

$$H = -\frac{1}{2}aT_cQ^2 + \frac{1}{4}b^*Q^4 + \frac{1}{6}c^*Q^6 \quad (5)$$

$$S = -\frac{1}{2}aQ^2. \quad (6)$$

There is a latent heat of transformation (for  $\beta \rightarrow \alpha$ ) of:

$$L = -\frac{1}{2}aT_{tr}Q_0^2. \quad (7)$$

To evaluate the role of strain and the evolution of the second order elastic constants, it is necessary to include strain terms explicitly. For the symmetry change  $P6_422 \leftrightarrow P3_221$  (or  $P6_222 \leftrightarrow P3_121$ ), the complete expansion is:

$$\begin{aligned} G = & \frac{1}{2}a(T - T_c)Q^2 + \frac{1}{4}bQ^4 + \frac{1}{6}cQ^6 + \frac{1}{8}dQ^8 \\ & + \lambda_1(e_1 + e_2)Q^2 + \lambda_3e_3Q^2 + \lambda_4(e_4^2 + e_5^2)Q^2 \\ & + \lambda_5(e_1e_4 - e_2e_4 + e_5e_6)Q + \lambda_6[e_6^2 + (e_1 - e_2)^2]Q^2 \\ & + \lambda_7(e_1 + e_2)Q^4 + \lambda_8e_3Q^4 + \lambda_9(e_1e_4 - e_2e_4 + e_5e_6)Q^3 \\ & + \frac{1}{4}(C_{11}^0 + C_{12}^0)(e_1 + e_2)^2 + \frac{1}{4}(C_{11}^0 - C_{12}^0)(e_1 - e_2)^2 \\ & + C_{13}^0(e_1 + e_2)e_3 + \frac{1}{2}C_{33}^0e_3^2 + \frac{1}{2}C_{44}^0(e_4^2 + e_5^2) + \frac{1}{2}C_{66}^0e_6^2. \end{aligned} \quad (8)$$

This differs from the expansions discussed previously (e.g., Höchli and Scott 1971 or Bachheimer and Dolino 1975) by the extension to eighth order in  $Q$ , the addition of the lowest order coupling terms permitted by symmetry for all six strains ( $e_1 - e_6$  in Voigt notation), and the inclusion of higher order coupling terms in  $e_1$ ,  $e_2$ , and  $e_3$ . The higher order terms are included in anticipation of the observation that the spontaneous strains  $e_1$  ( $= e_2$ ) and  $e_3$  do not vary linearly with  $Q^2$ . A coupling term of the form  $\lambda e_1^2 Q^2$  has the same symmetry properties as  $\lambda e_1 Q^4$  and is therefore equally valid for describing the higher order coupling but, along with  $\lambda e_3^2 Q^2$  for  $\lambda e_3 Q^4$ , leads to severe algebraic complexity. Rather than adding a higher

order coupling term, the non-linearity between strains and  $Q^2$  could have been accounted for by allowing the coefficients  $\lambda_1$  and  $\lambda_3$  to vary with temperature. However couplings of the form  $\lambda e Q^2$  lead to a renormalization of the fourth order coefficient of a Landau expansion, and this is not usually given an explicit temperature dependence. The higher order strain terms with constant coefficients  $\lambda_7$  and  $\lambda_8$  are therefore preferred at this stage. A higher order coupling term,  $\lambda_9 e_1 e_3 Q^3$ , has been added for completeness to produce a description of the anomalous behavior of  $C_{14}$  described by Höchli and Scott (1971). The angular strains  $e_4$ ,  $e_5$ , and  $e_6$  are strictly zero, by symmetry, but their coupling coefficients  $\lambda_4$ ,  $\lambda_5$ , and  $\lambda_6$  need not be zero, as discussed for variations of the elastic constants  $C_{14}$  ( $= -C_{24} = C_{56}$ ),  $C_{44}$  ( $= C_{55}$ ), and  $C_{66}$  in  $\alpha$  quartz. The superscript 0 on all the elastic constants in the full free energy expansion signifies that they are "bare" elastic constants. Their numerical values are such as to exclude the influence of the phase transition.

Under equilibrium conditions, a crystal must be at a free energy minimum with respect to strain, giving the formal conditions  $\partial G/\partial e_i = \partial G/\partial e_s = 0$ . Standard algebraic manipulations then yield:

$$e_3 = \frac{2\lambda_1 C_{13}^0 - \lambda_3 (C_{11}^0 + C_{12}^0)}{(C_{11}^0 + C_{12}^0)C_{33}^0 - 2C_{13}^0{}^2} Q^2 + \frac{2\lambda_7 C_{13}^0 - \lambda_8 (C_{11}^0 + C_{12}^0)}{(C_{11}^0 + C_{12}^0)C_{33}^0 - 2C_{13}^0{}^2} Q^4 \quad (9)$$

and:

$$(e_1 + e_2) = \frac{2\lambda_3 C_{13}^0 - 2\lambda_1 C_{33}^0}{(C_{11}^0 + C_{12}^0)C_{33}^0 - 2C_{13}^0{}^2} Q^2 + \frac{2\lambda_8 C_{13}^0 - 2\lambda_7 C_{33}^0}{(C_{11}^0 + C_{12}^0)C_{33}^0 - 2C_{13}^0{}^2} Q^4. \quad (10)$$

Substituting Equations 9 and 10 into Equation 8 (with  $e_4 = e_5 = e_6 = 0$ ) leads to relations between the fourth and sixth order coefficients,  $b$  and  $c$ , and their renormalized values,  $b^*$  and  $c^*$ , in Equation 1:

$$b^* = b - 2 \left[ \frac{\lambda_3^2 (C_{11}^0 + C_{12}^0) + 2\lambda_1^2 C_{33}^0 - 4\lambda_1 \lambda_3 C_{13}^0}{(C_{11}^0 + C_{12}^0)C_{33}^0 - 2C_{13}^0{}^2} \right] \quad (11)$$

$$c^* = c - 6 \{ [\lambda_3 \lambda_8 (C_{11}^0 + C_{12}^0) + 2\lambda_1 \lambda_7 C_{33}^0 - 2\lambda_1 \lambda_8 C_{13}^0 - 2\lambda_3 \lambda_7 C_{13}^0] / [(C_{11}^0 + C_{12}^0)C_{33}^0 - 2C_{13}^0{}^2] \}. \quad (12)$$

An eighth order term was not included in Equation 1, which is equivalent to assigning the value zero to the eighth order coefficient,  $d^*$ . The unrenormalized coefficient,  $d$ , in Equation 8 is not zero, and the two are related by:

$$d^* = d - 4 \left[ \frac{2\lambda_7^2 C_{33}^0 - 4\lambda_7 \lambda_8 C_{13}^0 + \lambda_8^2 (C_{11}^0 + C_{12}^0)}{(C_{11}^0 + C_{12}^0)C_{33}^0 - 2C_{13}^0{}^2} \right]. \quad (13)$$

Expressions for the isothermal (as opposed to adiabatic) elastic constants can be derived easily from Equation

8. The most general solution for systems in which the driving order parameter is not a symmetry breaking strain may be expressed as (after Slonczewski and Thomas 1970; Rehwald 1973; Bulou et al. 1992):

$$C_{ik} = \frac{\partial^2 G}{\partial e_i \partial e_k} - \sum_{m,n} \frac{\partial^2 G}{\partial e_i \partial Q_m} \left( \frac{\partial^2 G}{\partial Q_m \partial Q_n} \right)^{-1} \frac{\partial^2 G}{\partial e_k \partial Q_n}. \quad (14)$$

The order parameter is only one dimensional in the present case, so  $m = n = 1$ , and  $(\partial^2 G/\partial Q^2)^{-1}$  is referred to typically as the order parameter susceptibility,  $\chi$ . The general solution can therefore be simplified to:

$$C_{ik} = \frac{\partial^2 G}{\partial e_i \partial e_k} - \frac{\partial^2 G}{\partial e_i \partial Q} \chi \frac{\partial^2 G}{\partial e_k \partial Q}. \quad (15)$$

Consider  $C_{11}$ , for example. In  $\beta$  quartz  $Q = 0$  and, in the absence of thermal fluctuation effects,  $C_{11} = C_{11}^0$ ,  $C_{12} = C_{12}^0$ . For  $\alpha$  quartz the relevant symmetry-adapted forms of the elastic constants and strains are  $\frac{1}{2}(C_{11} + C_{12})$ ,  $\frac{1}{2}(C_{11} - C_{12})$ ,  $(e_1 + e_2)$ , and  $(e_1 - e_2)$ . The variations of  $(C_{11} + C_{12})$  and  $(C_{11} - C_{12})$  are given by:

$$\frac{1}{2}(C_{11} + C_{12}) = \frac{\partial^2 G}{\partial (e_1 + e_2)^2} - \left( \frac{\partial^2 G}{\partial (e_1 + e_2) \partial Q} \right)^2 \chi = \frac{1}{2}(C_{11}^0 + C_{12}^0) - [2\lambda_1 Q + 4\lambda_7 Q^3]^2 \chi \quad (16)$$

and

$$\frac{1}{2}(C_{11} - C_{12}) = \frac{\partial^2 G}{\partial (e_1 - e_2)^2} - \left( \frac{\partial^2 G}{\partial (e_1 - e_2) \partial Q} \right)^2 \chi = \frac{1}{2}(C_{11}^0 - C_{12}^0) + 2\lambda_6 Q^2. \quad (17)$$

$C_{11}$  and  $C_{12}$  can then be given separately as:

$$C_{11} = \frac{1}{2}(C_{11} + C_{12}) + \frac{1}{2}(C_{11} - C_{12}) = C_{11}^0 + 2\lambda_6 Q^2 - [2\lambda_1 Q + 4\lambda_7 Q^3]^2 \chi \quad (18)$$

and

$$C_{12} = \frac{1}{2}(C_{11} + C_{12}) - \frac{1}{2}(C_{11} - C_{12}) = C_{12}^0 - 2\lambda_6 Q^2 - [2\lambda_1 Q + 4\lambda_7 Q^3]^2 \chi. \quad (19)$$

Expressions for all the second-order elastic constants derived in this way are listed in Table 1. As expected for a system without any bilinear coupling between strain and the driving order parameter, deviations from the bare elastic constants are predicted to occur only in  $\alpha$  quartz.

Finally a general expression for the order parameter susceptibility can be derived from Equation 8 as:

$$\chi^{-1} = \frac{\partial^2 G}{\partial Q^2} = a(T - T_c) + 3bQ^2 + 5cQ^4 + 7dQ^6 + 2\lambda_1(e_1 + e_2) + 2\lambda_3 e_3 + 12\lambda_7(e_1 + e_2)Q^2 + 12\lambda_8 e_3 Q^2 + 2\lambda_4(e_1^2 + e_2^2) + 2\lambda_6[e_6^2 + (e_1 - e_2)^2] + 6\lambda_9(e_1 e_4 - e_2 e_4 + e_5 e_6)Q. \quad (20)$$

**TABLE 1.** Predicted variations (using Equations 8 and 15) for elastic constants of a material subject to a zone-center phase transition involving the symmetry change  $622 \approx 32$ 

$\beta$ quartz (622)	$\alpha$ quartz (32)
$C_{11} = C_{22} = C_{33}^0$	$C_{11} = C_{22} = C_{33}^0 + 2\lambda_6 Q^2 - [2\lambda_1 Q + 4\lambda_7 Q^3]^2 \chi$
$C_{33} = C_{33}^0$	$C_{33} = C_{33}^0 - [2\lambda_2 Q + 4\lambda_8 Q^3]^2 \chi$
$C_{12} = C_{12}^0$	$C_{12} = C_{12}^0 - 2\lambda_6 Q^2 - [2\lambda_1 Q + 4\lambda_7 Q^3]^2 \chi$
$C_{13} = C_{23} = C_{33}^0$	$C_{13} = C_{23} = C_{33}^0 - [2\lambda_1 Q + 4\lambda_7 Q^3][2\lambda_3 Q + 4\lambda_6 Q^3] \chi$
$C_{11} - C_{12} = C_{11}^0 - C_{12}^0$	$C_{11} - C_{12} = (C_{11}^0 - C_{12}^0) + 4\lambda_6 Q^2$
$C_{11} + C_{12} = C_{11}^0 + C_{12}^0$	$C_{11} + C_{12} = (C_{11}^0 + C_{12}^0) - 2[2\lambda_1 Q + 4\lambda_7 Q^3]^2 \chi$
$C_{14} = -C_{24} = C_{56} = 0$	$C_{14} = -C_{24} = C_{56} = \lambda_5 Q = \lambda_9 Q^3$
$C_{44} = C_{55} = C_{44}^0$	$C_{44} = C_{55} = C_{44}^0 + 2\lambda_4 Q^2$
$C_{66} = C_{66}^0 = \frac{1}{2}(C_{11}^0 - C_{12}^0)$	$C_{66} = C_{66}^0 + 2\lambda_6 Q^2 = \frac{1}{2}(C_{11} - C_{12})$

At equilibrium, the strains  $e_4$ ,  $e_5$ , and  $e_6$  are all zero and  $e_1 = e_2$ , giving:

$$\chi^{-1} = a(T - T_c) + (2b + b^*)Q^2 + \frac{1}{3}(8c + 7c^*)Q^4 + (4d + 3d^*)Q^6. \quad (21)$$

Over some temperature interval close to the transition point of a thermodynamically continuous phase transition, the Ginzburg interval, it is known that critical fluctuations must develop. However, for systems with significant spontaneous strains, this temperature interval is expected to be small (Ginzburg et al. 1987; Salje et al. 1992; Carpenter 1992; Salje 1993; and references therein). In the case of the  $\alpha \leftrightarrow \beta$  quartz transition, which has large strains and first-order character, a Ginzburg interval of  $|T_c - T_c| \ll 1$  K is likely. If deviations from the variations in physical properties predicted from Equation 8 are observed over a wider temperature range, it is most unlikely that critical fluctuations could be responsible.

### SPONTANEOUS STRAIN

The strains of interest for the present analysis are  $e_1$ ,  $e_3$ , and  $V_s$ , which are defined as:

$$e_1 = e_2 = \frac{a - a_0}{a_0} \quad (22)$$

$$e_3 = \frac{c - c_0}{c_0} \quad (23)$$

$$V_s = \frac{V - V_0}{V_0}. \quad (24)$$

Here  $a$ ,  $c$ , and  $V$  are lattice parameters of  $\alpha$  quartz at a given temperature, and  $a_0$ ,  $c_0$ , and  $V_0$  are reference parameters extrapolated down to the same temperature from the stability field of  $\beta$  quartz.

Two sets of high-temperature data were used to determine strains for a natural quartz sample from Brazil. The first set was obtained using the heating cell and INEL position sensitive detector system described by Salje et al. (1993). Approximately 35 powder diffraction lines (monochromatic  $\text{CuK}\alpha_1$  radiation) with  $2\theta$  values between  $21$  and  $114^\circ$  were used to refine the  $a$  and  $c$  lattice parameters.

Absolute temperature was not particularly well-con-

strained in these experiments, but was calibrated by choosing 847 K for the transition point evident in the data. The relative temperature scale was determined to a precision of about  $\pm 1$  K, using a thermocouple welded to the underside of the platinum heating strip on which the sample was placed. To constrain the extrapolation of  $a_0$ ,  $c_0$ , and  $V_0$  as precisely as possible, data collection was extended up to  $\sim 1340$  K, well into the stability field of  $\beta$  quartz.

The second data set was obtained by time-of-flight neutron powder diffraction at the ISIS facility. Data were collected for  $d$  spacings between  $0.7$  and  $2.5$  Å. Approximately  $5 \text{ cm}^3$  of the sample were held in a cylindrical vanadium can, and temperature was monitored using a thermocouple placed close to it. Measured temperatures were again rescaled by up to a few degrees to be consistent with a transition temperature of 847 K. For data below room temperature, the sample was held in a helium-flow cryostat. The two sets of lattice parameters listed in Table 2 are illustrated in Figure 1. Greater scatter in the X-ray data is a consequence of the poorer resolution of the position sensitive detector relative to that of the neutron diffractometer.

Extrapolations of  $a_0$ ,  $c_0$ , and  $V_0$  from linear least-squares fits to the combined X-ray and neutron data above  $T_c$  are described by  $a_0 = 4.996 + 2.63 \times 10^{-6}T$  (Å),  $c_0 = 5.464 - 5.63 \times 10^{-6}T$  (Å), and  $V_0 = 118.15 - 3.64 \times 10^{-5}T$  (Å<sup>3</sup>), for  $T$  in Kelvins. The resulting strains, calculated using Equations 22–24, are shown in Figure 2. Coupling of the form  $\lambda e Q^2$  should normally lead to strain-order parameter relationships of the form  $e \propto Q^2$ . Also, for trigonal and hexagonal systems,  $V_s = 2e_1 + e_3$  to a good approximation. The strain data might at first be expected to vary as  $e_1 \propto e_3 \propto V_s \propto Q^2$ . If this is the case, the equilibrium variation of  $Q^2$  can be determined by substituting  $V_s$  for  $Q^2$  in Equation 2:

$$V_s = \frac{2}{3}V_{s,0} \left\{ 1 + \left[ 1 - \frac{3}{4} \left( \frac{T - T_c}{T_c - T_c} \right) \right]^{1/2} \right\}. \quad (25)$$

The constant of proportionality between  $V_s$  and  $Q^2$  cancels out because it appears on both sides of the equation, and  $V_{s,0}$  specifies the magnitude of the discontinuity in  $V_s$  at  $T = T_c$ . The value of  $T_c = 847$  K was chosen because it falls within the hysteresis limits of  $\sim 845.7$  K (incommensurate phase  $\rightarrow \alpha$  quartz) and  $\sim 847.2$  K ( $\alpha$  quartz  $\rightarrow$

TABLE 2. Lattice parameters as a function of temperature for quartz

Neutron data				X-ray data			
$T$ (K)	$a$ (Å)	$c$ (Å)	$V$ (Å <sup>3</sup> )	$T$ (K)	$a$ (Å)	$c$ (Å)	$V$ (Å <sup>3</sup> )
4	4.90158	5.39896	112.334	293	4.9135(3)	5.4042(5)	113.01(1)
25	4.90160	5.39898	112.336	321	4.9150(3)	5.4058(6)	113.09(2)
50	4.90189	5.39907	112.351	346	4.9172(4)	5.4069(8)	113.22(2)
75	4.90249	5.3993	112.383	370	4.9186(4)	5.4090(8)	113.35(2)
100	4.90326	5.39965	112.426	389	4.9216(5)	5.4083(8)	113.45(2)
125	4.90423	5.40011	112.480	408	4.9223(3)	5.4095(7)	113.51(2)
150	4.90532	5.40068	112.542	428	4.9231(4)	5.4105(9)	113.56(2)
175	4.90651	5.40132	112.610	447	4.9254(8)	5.4110(13)	113.68(3)
200	4.90779	5.40201	112.683	466	4.9268(7)	5.4129(12)	113.79(2)
225	4.90922	5.40283	112.766	486	4.9292(5)	5.4139(10)	113.92(2)
250	4.91071	5.40370	112.852	505	4.9308(5)	5.4164(9)	114.05(3)
308	4.91478	5.40620	113.092	524	4.9339(6)	5.4172(10)	114.20(3)
383	4.91995	5.40916	113.392	544	4.9353(5)	5.4190(10)	114.31(2)
434	4.92406	5.41173	113.635	563	4.9363(5)	5.4211(10)	114.40(2)
484	4.92851	5.41454	113.900	583	4.9397(6)	5.4227(11)	114.59(3)
524	4.93220	5.41688	114.120	602	4.9416(6)	5.4243(11)	114.71(3)
564	4.93602	5.41933	114.348	622	4.9438(5)	5.4247(10)	114.82(2)
605	4.94027	5.42203	114.602	641	4.9458(5)	5.4269(9)	114.96(2)
645	4.94506	5.42509	114.890	660	4.9473(4)	5.4278(7)	115.05(2)
670	4.94961	5.42835	115.170	680	4.9498(3)	5.4305(7)	115.23(2)
700	4.95297	5.43048	115.372	699	4.9523(4)	5.4311(8)	115.35(2)
720	4.95565	5.43212	115.532	718	4.9574(5)	5.4316(10)	115.60(2)
739	4.95857	5.43407	115.709	738	4.9603(5)	5.4345(10)	115.80(2)
761	4.96180	5.43608	115.903	757	4.9626(6)	5.4375(9)	115.97(2)
781	4.96534	5.43835	116.117	776	4.9664(6)	5.4423(11)	116.25(3)
816	4.97424	5.44404	116.656	796	4.9684(7)	5.4455(9)	116.42(3)
824	4.97722	5.44599	116.837	805	4.9702(7)	5.4468(11)	116.53(3)
832	4.98081	5.44828	117.055	815	4.9746(7)	5.4451(10)	116.69(3)
841	4.98624	5.45169	117.384	825	4.9785(7)	5.4459(10)	116.90(3)
848	4.99672	5.45768	118.007	834	4.9819(6)	5.4487(8)	117.10(3)
851	4.99795	5.45892	118.092	844	4.9904(14)	5.4487(21)	117.51(7)
853	4.99803	5.45894	118.096	854	4.9966(5)	5.4567(9)	117.89(2)
855	4.99809	5.45897	118.100	864	4.9981(5)	5.4584(8)	118.09(2)
857	4.99816	5.45896	118.103	873	4.9983(5)	5.4579(7)	118.09(2)
859	4.99819	5.45906	118.107	893	4.9988(4)	5.4589(7)	118.13(2)
861	4.99828	5.45896	118.109	912	5.0002(5)	5.4595(11)	118.21(3)
866	4.99839	5.45901	118.115	931	5.0001(6)	5.4606(10)	118.23(2)
871	4.99846	5.45903	118.119	950	4.9994(5)	5.4590(9)	118.16(2)
876	4.99852	5.45902	118.121	999	5.0003(4)	5.4587(8)	118.20(2)
881	4.99861	5.45894	118.124	1047	4.9987(8)	5.4566(14)	118.08(3)
				1095	4.9998(5)	5.4568(10)	118.14(2)
				1145	4.9990(6)	5.4569(10)	118.10(2)
				1193	5.0008(5)	5.4564(11)	118.17(3)
				1241	5.0004(5)	5.4554(10)	118.13(2)
				1289	4.9990(7)	5.4588(13)	118.07(3)
				1338	4.9976(7)	5.4559(13)	118.01(3)

Note: Figures in brackets represent the uncertainties ( $1\sigma$ ) in the last figure of the quoted lattice parameters for the X-ray data (derived from the least squares fitting procedure). The equivalent uncertainty in the neutron data is estimated as  $\pm 1$  in the last figure.

$\beta$  quartz) from experiments in which temperature was well-constrained (Dolino et al. 1984). It is also within  $\sim 1$  K of most of the transition temperatures listed in Ghiorso et al. (1979).

Attempts to fit the parameters in Equation 25 using  $V_s$  data gave strong correlations between  $T_c$  and  $V_{s,0}$ . An independent determination of  $V_{s,0}$  was therefore adopted, on the basis of the high-precision thermal expansion data reported by Bachheimer (1980, 1986) and Mogeon (1988) for temperatures within  $\sim 2$  K of the transition. At the midpoint between the hysteresis limits, their results give the difference in linear strain between  $\beta$  quartz (extrapolated from the  $\beta$  stability field into the stability field of the incommensurate structure) and  $\alpha$  quartz as  $-2.1 \times 10^{-3}$ ,  $-1.9 \times 10^{-3}$ , and  $-2.0 \times 10^{-3}$ , respectively. From correlations of  $e_1$  with  $V_s$  and  $e_3$ , an average value of  $e_{1,0}$

$= -2.0 \times 10^{-3}$  corresponds to  $V_{s,0} = -5.1 \times 10^{-3}$  and  $e_{3,0} = -1.1 \times 10^{-3}$ . Refitting the neutron data in the temperature interval 308 – 841 K with  $T_c$  as the only variable then yielded  $T_c = 843.9$  K. The fit is shown in Figure 2, as are variations of  $e_3$  and  $e_1$  using the corresponding  $e_{3,0}$ ,  $e_{1,0}$  values and the same  $T_{tr}$ ,  $T_c$  values. Agreement between the observed and fit variations is reasonable, except for the marked deviation of  $e_3$  below  $\sim 650$  K. (Note that strain data from below room temperature were not included in the fitting process because of the effects of order parameter saturation. These have been described by Salje et al. 1991 and are not accounted for by the standard Landau expansion).

Values of  $T_{tr} - T_c$  were determined in several studies and are typically in the range 4–13 K (Axe and Shirane 1970; Höchli and Scott 1971; Grimm and Dorner 1975;

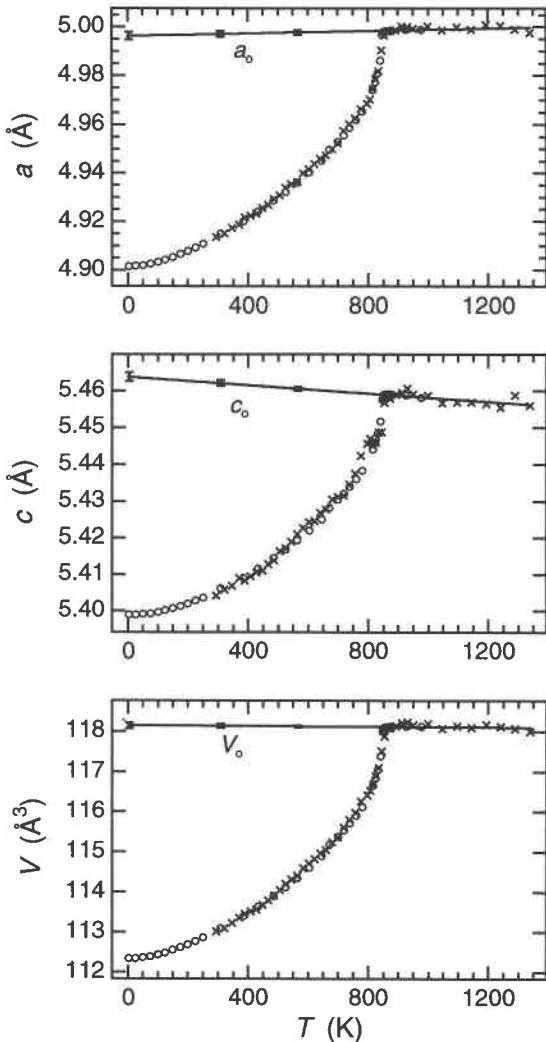


FIGURE 1. Lattice parameters of quartz from X-ray powder diffraction data (crosses) and neutron powder diffraction data (open circles). The values for  $a_0$ ,  $c_0$ , and  $V_0$  are the parameters of  $\beta$ -quartz extrapolated from high temperatures into the stability field of  $\alpha$  quartz. Uncertainties in  $a_0$  (derived from  $\pm 1\sigma$  in the fit parameters) are shown for three temperatures.

Bachheimer and Dolino 1975; Banda et al. 1975; Boysen et al. 1980; Tezuka et al. 1991; Dolino et al. 1992; Kihara 1993). The value of 3.1 K from the strain data thus appears to be somewhat low. A small non-linearity in the relationship between  $e_1$  and  $e_3$  (Fig. 3) suggests that a factor in the inconsistency could be the existence of higher order strain-order parameter coupling effects. This possibility appears to be confirmed by comparing the observed spontaneous strains with independently determined values of the order parameter.

The most tightly constrained determination currently available for  $Q$  in the temperature interval 298–846 K is given by Bachheimer and Dolino (1975) from optical data. Their best fit to Equation 2 gave  $T_{tr} - T_c = 7.2$  K. This has been rounded to 7 K here. For  $T_{tr} = 847$  K,  $T_c$

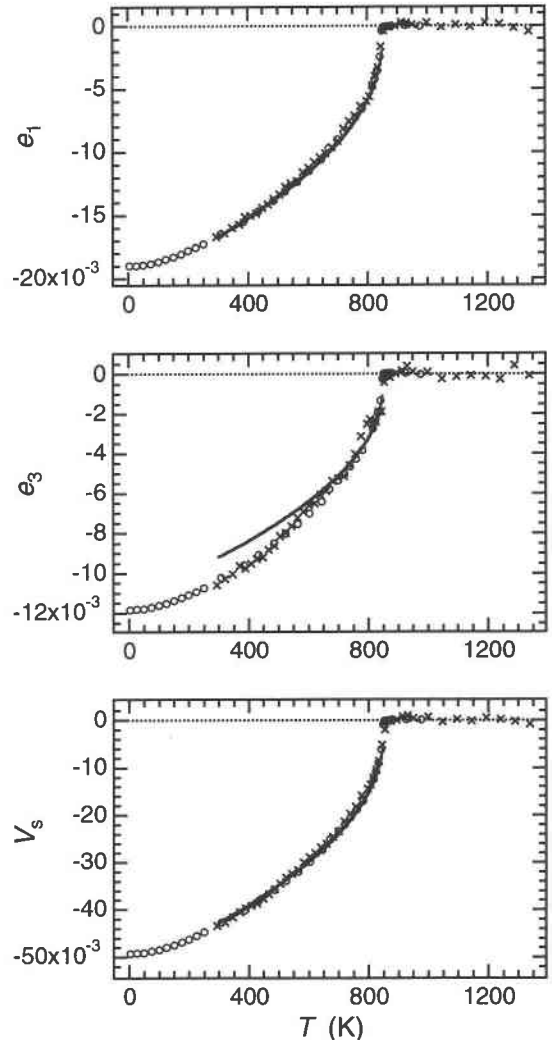


FIGURE 2. Strains calculated using Equations 22–24 (symbols as in Fig. 1). The curves are solutions to Equation 25 with  $T_{tr} = 847$  K,  $T_c = 843.9$  K,  $e_{1,0} = -0.0020$ ,  $e_{3,0} = -0.0011$ ,  $V_{s,0} = -0.0051$ . The main source of uncertainty in strains from the neutron data derives from the extrapolations of  $a_0$ ,  $c_0$ , and  $V_0$ . Propagation of  $\pm 1\sigma$  for the fit parameters of these gives uncertainties that are smaller than the dimensions of the symbols at temperatures above  $\sim 300$  K.

is therefore 840 K, which is within uncertainty limits of the experimental value of 841 K determined by Tezuka et al. (1991). According to Equations 9 and 10, higher order strain coupling terms of the form  $\lambda eQ^4$  in the Landau expansion should lead to relationships of the form:

$$e_i = AQ^2 + BQ^4 \quad (26)$$

for  $i = 1 - 3$ . The linear strains have therefore been plotted against  $Q^2$ , as calculated from Equation 2 with  $T_{tr} = 847$  K,  $T_c = 840$  K, and  $Q_0 = 0.377$  (Fig. 4). (The value of  $Q_0$  is obtained by using these values of  $T_{tr}$  and  $T_c$  with  $Q = 1$  at 0 K). A standard least-squares fitting procedure for the neutron diffraction results yielded the

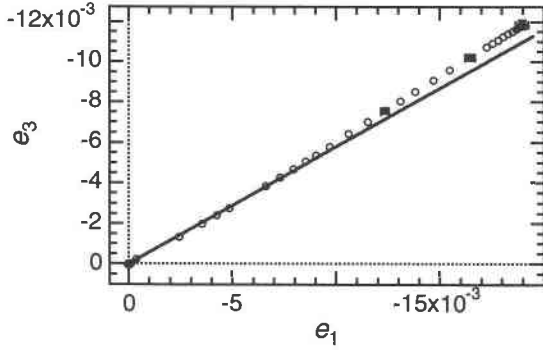


FIGURE 3. Variation of  $e_3$  with  $e_1$  for strains derived from the neutron diffraction data. The straight line passing through the origin is a guide to the eye, drawing attention to a non-linear relationship between the two strains. Propagated uncertainties (from  $\pm 1\sigma$  in the fit parameters for  $a_0$  and  $c_0$ ) are shown for points corresponding to 565, 308, and 4 K.

values  $A = -0.01656$ ,  $B = -0.00501$  for  $e_1$ , and  $A = -0.00900$ ,  $B = -0.00476$  for  $e_3$ . As before, data for  $T < 298$  K were excluded from the fit. From Figure 4 it is evident that a reasonable match with the data is obtained for  $0.25 \leq Q^2 \leq 0.8$ . Observed strains from temperatures within  $\sim 25$  K of the transition point fall slightly below the curve, as is seen more clearly in Figure 5 where the same results are plotted against temperature instead of  $Q^2$ . The discontinuities in  $e_1$  and  $e_3$  at 847 K from the fits are  $e_{1,0} = -0.0024$ ,  $e_{3,0} = -0.0014$ , i.e., slightly larger than the values of  $e_{1,0}$  and  $e_{3,0}$  derived above from the measurements of Bachheimer (1980, 1986) and Mogeon (1988). Lattice parameter data at smaller temperature intervals through the transition are needed to establish the precise topology of the  $\alpha$  quartz curves as  $T \rightarrow T_r$  and to show whether the single neutron data point for  $\beta$  quartz that suggests a significant strain ahead of the transition is real.

As an aside, Levanyuk et al. (1993) have suggested that, because of the effect of fluctuations, odd order terms can appear in Landau free energy expansions for transitions in which they would be otherwise be expected to be forbidden by symmetry. The data for  $e_1$  were therefore also considered in the light of a Landau expansion of the form:

$$G = \frac{1}{2}a(T - T_c)Q^2 + \frac{1}{3}u|Q|^3 + \frac{1}{4}bQ^4. \quad (27)$$

In this case the equilibrium variation of  $Q$  is given by:

$$Q = \frac{3}{4}Q_0 \left\{ 1 + \left[ 1 - \frac{8}{9} \left( \frac{T - T_c}{T_r - T_c} \right)^{1/2} \right] \right\}. \quad (28)$$

The predicted variation of  $e_1$  becomes:

$$(e_1)^{1/2} = \frac{3}{4}(e_{1,0})^{1/2} \left\{ 1 + \left[ 1 - \frac{8}{9} \left( \frac{T - T_c}{T_r - T_c} \right)^{1/2} \right] \right\}. \quad (29)$$

If  $e_{1,0} = -2.0 \times 10^{-3}$  and  $T_r = 847$  K as before, the resulting fit is very poor and gives an unrealistic value of

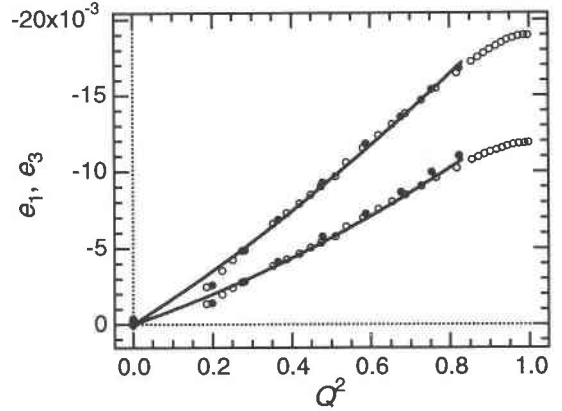


FIGURE 4. Variations of  $e_1$  and  $e_3$  (from neutron diffraction data) as a function of  $Q^2$  calculated for  $T_r = 847$  K,  $T_c = 840$  K. The curves are fits to the data between 308 and 841 K using an equation of the form of Equation 26. Strains calculated from the high-temperature lattice parameter data of Kihara (1990) are also shown for comparison (filled circles).

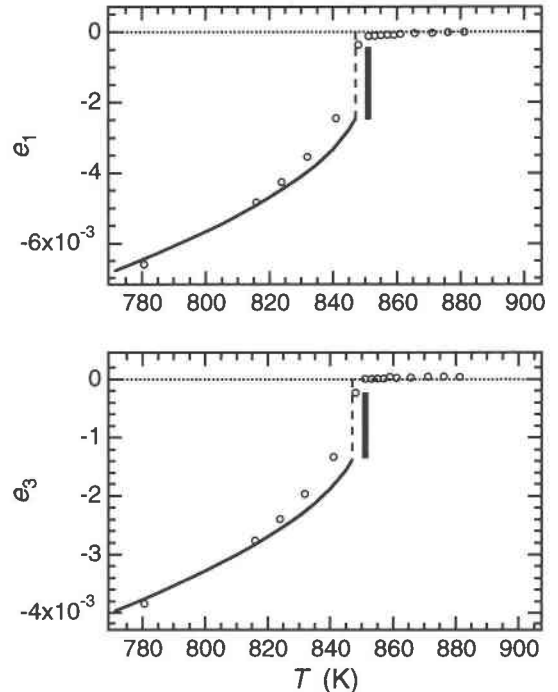


FIGURE 5. Strain variations (from neutron diffraction data) in the vicinity of the transition temperature. The curves are derived from Equation 26 with the coefficients from the fits shown in Figure 4. Note that the experimental data points just below the transition temperature fall below the Landau solution, and there may be a small dip in the strain as  $T_r$  is approached from above. The solid bars represent the magnitudes of the discontinuities expected on the basis of the linear expansion data of Bachheimer (1980, 1986) and Mogeon (1988).

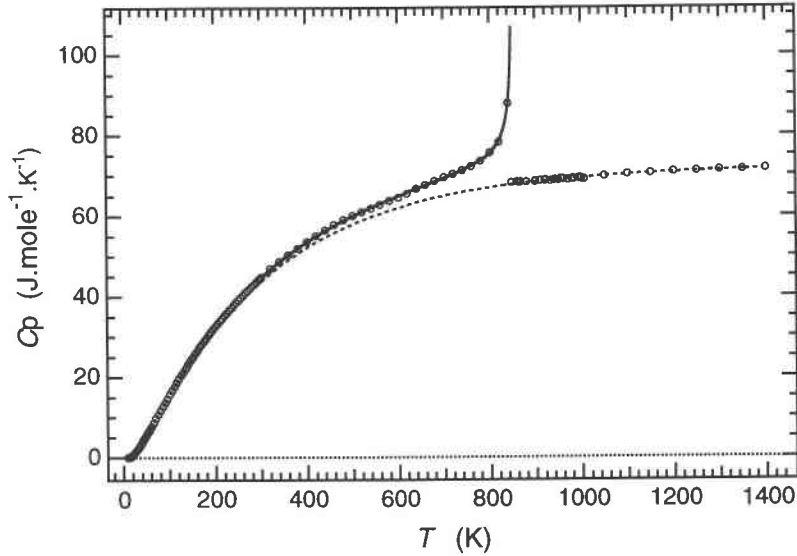


FIGURE 6. Variations of heat capacity for quartz (data from Gurevich and Khlyustov 1979; Grønvold et al. 1989). The broken line represents the heat capacity of  $\beta$  quartz (Eq. 36), and the solid line represents the heat capacity of  $\alpha$  quartz. The difference between the two curves is the excess heat capacity,  $\Delta C_p$ , associated with the phase transition.

$T_c \approx 800$  K. The experimental data alone do not prove that a third-order term is zero but, if it exists in an otherwise standard 246 potential, it is presumably small.

The volume strain at  $T_r$  is given by  $2e_{1,0} + e_{3,0}$  and, from the fit between  $Q^2$  and the strains, is  $-6.3 \times 10^{-3}$ . Taking the unit-cell volume of  $\beta$  quartz as being  $118.1 \text{ \AA}^3$  at 847 K gives a volume discontinuity of  $-0.744 \text{ \AA}^3$ . This corresponds to a molar volume reduction of  $0.149 \text{ cm}^3$ . The more direct measurement of this discontinuity from the macroscopic linear strain measurements of Bachheimer (1980, 1986) and Mogeon (1988),  $-5.1 \times 10^{-3}$ , gives  $0.121 \text{ cm}^3/\text{mol}$ . Both values fall within the range  $0.11\text{--}0.21 \text{ cm}^3/\text{mol}$  reported in the literature (see compilation in Table 7 of Ghiorso et al. 1979).

#### CALIBRATION OF LANDAU COEFFICIENTS USING $C_p$ DATA

Fitting the solution for  $Q$  as a function of  $T$  to some set of data that is directly related to the driving order parameter yields ratios between the Landau coefficients but not their absolute values. A further measurement is always needed, and for rapid structural phase transitions, a useful property that can be measured with high precision is the excess heat capacity,  $\Delta C_p$ . In all Landau expansions of the type used above, only the *excess* free energy, entropy and entropy are specified, and it is often convenient to drop the prefix  $\Delta$ . To avoid ambiguity the prefix is retained in this section, however.

By definition,  $\Delta C_p$  of the transition is related to the excess entropy  $\Delta S$  ( $= S$  in Eq. 6) by:

$$\Delta C_p = T \frac{\partial \Delta S}{\partial T}. \quad (30)$$

Combining Equations 2, 6, and 7 gives:

$$\Delta S = \frac{2}{3} \frac{L}{T_r} \left\{ 1 + \left[ 1 - \frac{3}{4} \left( \frac{T - T_c}{T_r - T_c} \right) \right]^{3/2} \right\}. \quad (31)$$

Differentiation of Equation 31 with respect to  $T$  and substitution into Equation 30 yields, after some algebraic manipulation (see also, Aleksandrov and Flerov 1979; Salje 1993):

$$\begin{aligned} \left( \frac{T}{\Delta C_p} \right)^2 &= \frac{64(T_r - T_c)^2}{a^2 Q_0^4} \left[ 1 - \frac{3}{4} \left( \frac{T - T_c}{T_r - T_c} \right) \right] \\ &= \frac{64(T_r - T_c)^2}{a^2 Q_0^4} + \frac{48(T_r - T_c)T_c}{a^2 Q_0^4} \\ &\quad - \frac{48(T_r - T_c)T}{a^2 Q_0^4}. \end{aligned} \quad (32)$$

A plot of the left hand side of this equation against  $T$  should yield a straight line with slope  $[-48(T_r - T_c)/a^2 Q_0^4]$ . In the present case,  $T_r$ ,  $T_c$ , and  $Q_0$  are all known, so the value of  $a$  can be determined.

Selected  $C_p$  data for quartz are shown in Figure 6. The data for  $T \leq 298$  K are from Gurevich and Khlyustov (1979). The higher temperature data are from Grønvold et al. (1989), including points from their Table 6 for  $T \leq 1400$  K, and points from their Table 1 (series III, VIII), and their Table 3 for  $860 \text{ K} \leq T \leq 1005$  K. A polynomial of the form:

$$C_p = \alpha + \beta T + \gamma T^2 + \delta T^3 \quad (33)$$

was fit to the data between 900 and 1400 K giving the coefficients  $\alpha = 31.16$ ,  $\beta = 0.07889$ ,  $\gamma = -5.311 \times 10^{-5}$ ,  $\delta = 1.235 \times 10^{-8}$ , for  $C_p$  in  $\text{J}/(\text{mol}\cdot\text{K})$ . This parameterized curve was then extrapolated into the stability field of  $\alpha$  quartz to allow the difference  $\Delta C_p = C_p(\alpha \text{ quartz}) - C_p(\beta \text{ quartz})$  to be determined as a function of temperature.



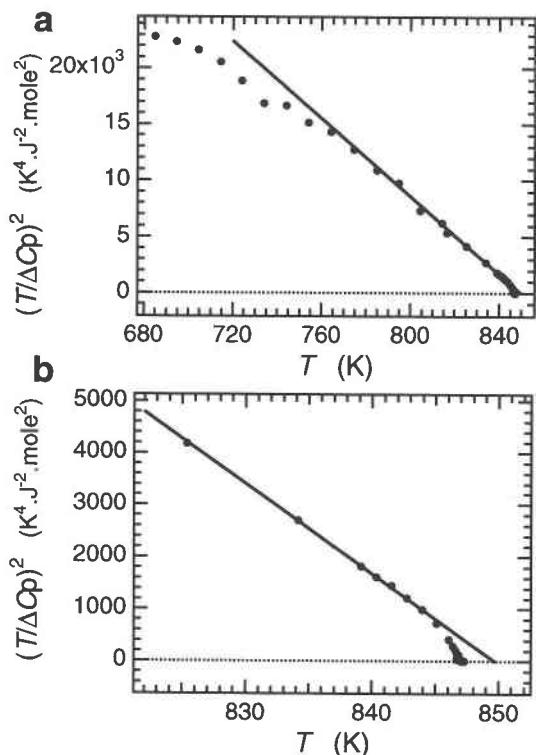


FIGURE 7. Plot of excess heat capacity variation based on Equation 32. The straight line is a least-squares fit to the data between 825 and 845 K. An expanded region around  $T_r$  in (a) is shown in (b). The straight line extrapolates to zero at  $T_1 = 849.7$  K.

Figure 7 shows the plots suggested by Equation 32 using these values for  $\Delta C_p$ . It should be anticipated that uncertainties in  $\Delta C_p$  increase with increasing extrapolation of the  $\beta$  quartz curve into the  $\alpha$  quartz field. This is reflected in the increasing divergence shown in Figure 7a, though the fit remains consistent with the data down to  $\sim 760$  K. Similarly, the uncertainties in  $C_p$  for  $\alpha$  quartz increase as the transition point is approached from below because the equilibrium heat capacity curve becomes steep. In the close vicinity of the transition point other factors, such as critical fluctuations or the presence of defects, can have a significant effect on  $\Delta C_p$  (e.g., Salje 1988). The slope used to calculate a value of the  $a$  coefficient was therefore determined by least-squares fitting to values of  $(T/\Delta C_p)^2$  between 825 and 845 K. Only data from within  $\sim 1$  K of the transition point fall off this line and it also matches data down to  $\sim 760$  K.

The slope of the linear fit shown in Figure 7b is  $-173.0 \text{ mol}^2 \cdot \text{K}^3/\text{J}^2$  that, from the slope term in Equation 32 and values of  $T_r - T_c = 7$ ,  $Q_0 = 0.377$ , yields  $a = 9.8 \text{ J}/(\text{mol} \cdot \text{K})$ . Equation 3 then yields  $b^* = -1931 \text{ J}/\text{mol}$  and Equation 4 yields  $c^* = 10\,190 \text{ J}/\text{mol}$ . (Note that the statistically unrealistic number of significant figures for the values of  $b^*$  and  $c^*$  is retained here to avoid subsequent rounding errors).

An important test for internal consistency is a compar-

ison of the values of  $T_r - T_c$  with the extrapolated temperature,  $T_1$ , at which  $(T/\Delta C_p)^2$  goes to zero. These three temperatures are related in a standard way for first-order transitions described by Equation 1 (easily derived from Equation 32, or see Bachheimer and Dolino 1975):

$$(T_r - T_c) = 3(T_1 - T_r). \quad (34)$$

Physically,  $T_1$  is the upper temperature limit for the metastable persistence of  $\alpha$  quartz with respect to  $\beta$  quartz (the local minimum at  $Q \neq 0$  in the free energy curve,  $G(Q)$ , at  $T_1 > T > T_r$  becomes a saddle point at  $T = T_1$ ). For  $T_r = 847$  K and  $T_r - T_c = 7$  K,  $T_1$  would be 849.3 K, which is in adequate agreement with  $T_1 = 849.7$  K from the linear fit shown in Figure 7b.

A second test is a comparison of calculated and observed latent heats for the transition. If  $a = 9.8 \text{ J}/(\text{mol} \cdot \text{K})$ ,  $T_r = 847$  K and  $Q_0 = 0.377$ , then Equation 7 gives the magnitude of the latent heat as 590 J/mol. This value should be slightly greater than the observed value because the actual transition is between  $\alpha$  quartz and the incommensurate structure rather than directly between the  $\alpha$  and  $\beta$  forms. Other experimental determinations of the latent heat are spread over a range from  $\sim 400$  to  $\sim 800$  J/mol (summarized in Table 6 of Ghiorso et al. 1979), largely because of the inherent difficulty in measuring any latent heat directly. Richet et al. (1982) quoted 655 J/mol and Drebuschak and Dement'ev (1993) gave 300–400 J/mol. The Landau entropy change,  $S_0$  at  $T = T_r$ , is 0.696 J/(mol·K) (from Equation 6 with  $Q_0 = 0.377$ ). Dorogokupets (1995) gave 0.335 J/(mol·K). Taking the Clapeyron Equation as  $dP/dT = S_r/V_{s,0}$  yields a  $P$ - $T$  slope of 47 bar/K for the  $\alpha \leftrightarrow \beta$  transition at 1 bar (using  $V_{s,0} = -6.3 \times 10^{-3}$ ) that, again, falls within the experimental range of 35–65 bar/K (Ghiorso et al. 1979).

A third comparison is with a hypothetical configurational change in relation to the controversy as to whether the transition is displacive or order-disorder in character (reviewed most recently by Heaney and Veblen 1991; Kihara 1993; Dolino and Vallade 1994; Heaney 1994). The value of  $a = 9.8 \text{ J}/(\text{mol} \cdot \text{K})$  implies an excess entropy for the change from  $Q = 0$  to  $Q = 1$  of  $-4.9 \text{ J}/(\text{mol} \cdot \text{K})$  (Eq. 6). If the transition was purely order-disorder in character, with each tetrahedron in  $\alpha$  quartz being ordered and each tetrahedron of  $\beta$  quartz being fully disordered between two orientations, there would be a configurational entropy change  $S_{\text{config}} = -R(\frac{1}{2}\ln\frac{1}{2} + \frac{1}{2}\ln\frac{1}{2}) = -5.76 \text{ J}/(\text{mol} \cdot \text{K})$ . These two entropies are sufficiently close as to be consistent with order-disorder behavior but do not preclude displacive character for the phase transition.

The excess heat capacity of  $\alpha$  quartz with respect to  $\beta$  quartz is given by:

$$\left(\frac{T}{\Delta C_p}\right)^2 = 1.47 \times 10^5 - 173.0 T \quad (35)$$

which is the linear fit shown in Figure 7b.  $C_p$  for  $\beta$  quartz can therefore be determined at any temperature below  $T_r$  simply by subtracting the Landau  $\Delta C_p$  value from the observed  $C_p$  values of  $\alpha$  quartz. A fit to the resulting  $C_p$

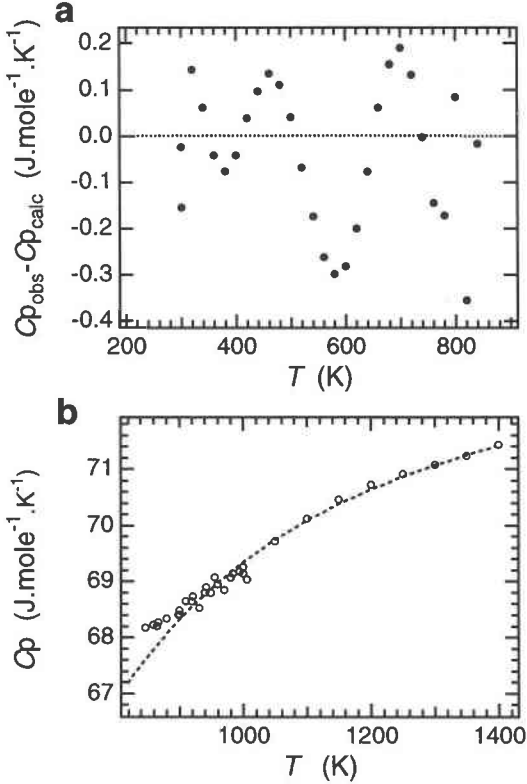


FIGURE 8. (a) Differences between the observed and calculated values of  $C_p$  for  $\alpha$  quartz. The calculated values are given by  $C_p$  for  $\beta$  quartz from Equation 36 plus  $\Delta C_p$  for the transition from Equation 35. (b) Comparison between  $C_p$  data for  $\beta$  quartz and the fit given by Equation 36. In a narrow temperature interval above the transition point there is a small anomaly not accounted for by the fit.

curve in the temperature range 300–1400 K, but excluding data for 840–900, is shown as a dotted line in Figure 6. It is described in a standard form by:

$$C_p(\beta\text{-quartz}) = 168.9 - 0.04064 T + 8.567 \times 10^{-6} T^2 - 2166 T^{-1/2} + 1.023 \times 10^6 T^{-2} \quad (36)$$

Adding  $\Delta C_p$  from Equation 35 to  $C_p$  ( $\beta$  quartz) in Equation 36 gives the resulting curve for  $C_p$  ( $\alpha$  quartz) shown in Figure 6. Differences between the observed and calculated values of  $C_p$  for  $\alpha$  quartz are shown in Figure 8a.  $C_p$  for  $\beta$  quartz could be determined for  $T < 300$  K in the same way, but the Landau solution used here does not take into account the effect of order parameter saturation.  $\Delta C_p$  is not likely to be correct quantitatively in this interval.

Finally, Figure 8b shows a small tail in  $C_p$  above the transition point, which is not accounted for in the present analysis. A discrepancy of less than 1 J/(mol·K) remains between the fit for  $\beta$  quartz (Eq. 36) and the observed heat capacities, and presumably this reflects structural changes ahead of the phase transition.

### ELASTIC CONSTANT VARIATIONS AT $T > T_t$

The observed elastic constant variations of quartz between  $\sim 300$  and  $\sim 1100$  K are shown in Figure 9 (data from Atanasoff and Hart 1941; Atanasoff and Kammer 1948; Kammer et al. 1948; Zubov and Firsova 1962; Shapiro and Cummins 1968; Höchli 1970; Pelous and Vacher 1976; Unoki et al. 1984; Ohno 1995). In the stability field of  $\beta$  quartz,  $C_{44}$  and  $C_{66}$  hardly vary at all with temperature, whereas  $C_{11}$ ,  $C_{33}$ ,  $C_{13}$ , and  $C_{12}$  show a marked softening as  $T \rightarrow T_t$ . Elastic softening can occur as a transition point is approached from the high symmetry side in systems where the relevant spontaneous strains are coupled bilinearly with the driving order parameter. This softening is not possible when the lowest order couplings are of the form  $\lambda e Q^2$ , as in the present case (Eq. 8). The observed softening cannot be due to critical fluctuations of the order parameter because it occurs over a temperature interval of apparently  $\sim 200$  K. Rather it conforms to a pattern also found in the high symmetry phases of gadolinium molybdate (Höchli 1972) terbium molybdate (Yao et al. 1981) and  $KMnF_3$  perovskite (Cao and Barsch 1988).

Following the theoretical analysis of Pytte (1970, 1971) and Axe and Shirane (1970), elastic softening in the high symmetry phase ahead of an improper ferroelastic or co-elastic transition has been considered in terms of the effects of coupling between different vibrational modes (Höchli 1972; Rehwald 1973; Cummins 1979; Lüthi and Rehwald 1981; Yao et al. 1981; Fossum 1985; Carpenter and Salje, unpublished manuscript). The underlying physical picture is the following: Associated with a soft mode at some specific point in reciprocal space, there is a set of branches that also soften to some extent. Just as with the soft mode itself, the amplitudes of modes along the soft branches should increase as their frequencies decrease. They can combine to produce stress fluctuations and, hence, strain fluctuations. The summation of all such combinations yields a net softening of some specific acoustic modes and this is manifested as a softening of the related elastic constants. The total effect should increase as the amplitudes of the modes increase, reaching a maximum at the transition point. The temperature dependence of this fluctuation-induced softening is generally described by:

$$C_{ik} - C_{ik}^0 = \Delta C_{ik} = A_{ik} |T - T_c|^{K_{ik}} \quad (37)$$

$A_{ik}$  and  $K_{ik}$  are properties of the material of interest; their subscripts are retained as labels to match with the corresponding  $C_{ik}$  terms. The values of  $K_{ik}$  are sensitive both to the degree of anisotropy of dispersion curves about the reciprocal lattice vector of the soft mode and to the extent of softening along each branch (Axe and Shirane 1970; Pytte 1970, 1971; Höchli 1972; Carpenter and Salje, unpublished manuscript). There are symmetry constraints limiting which elastic constants can soften by this mechanism. First, the effect should be restricted to those elastic constants that transform (in the group theoretical sense)

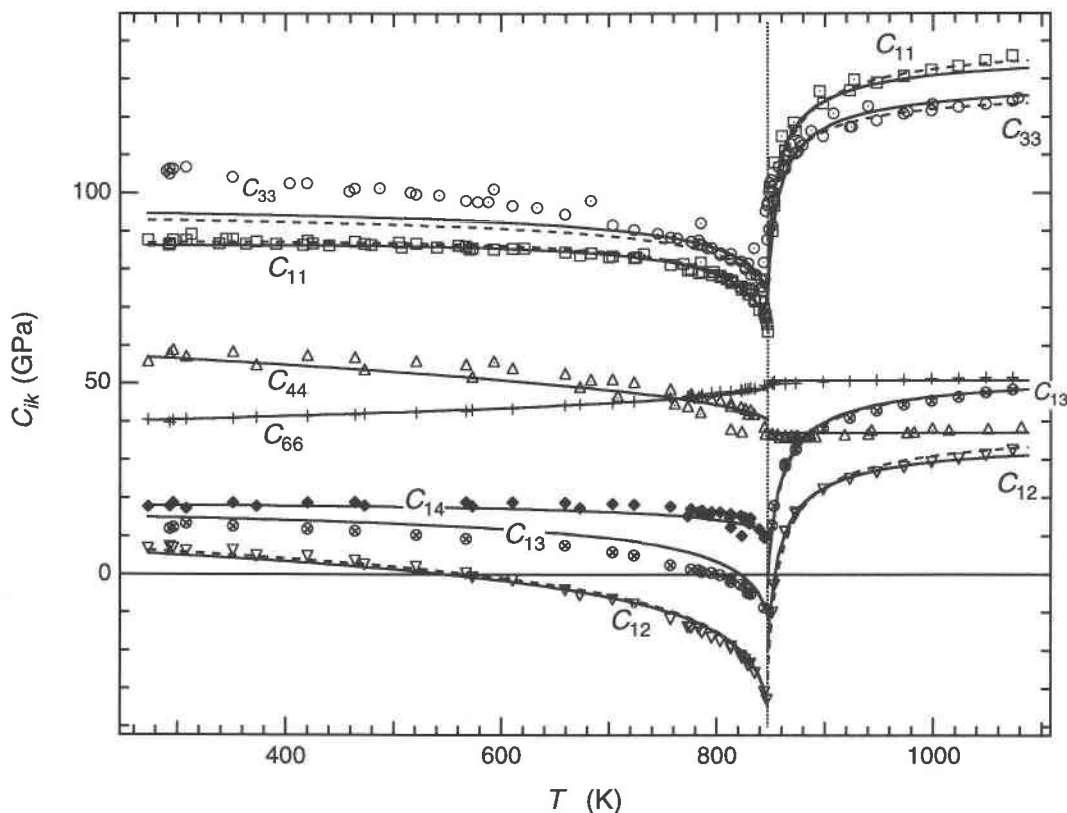


FIGURE 9. Comparison between observed and calculated elastic constant variations for quartz. For  $C_{11}$ ,  $C_{33}$ , and  $C_{44}$  a distinction has been made between data from ultrasonic experiments (open symbols) and data from Brillouin scattering experiments (open symbols containing a dot). References to the sources of data are given in the text. Two sets of calculated variations are

shown for  $C_{11}$ ,  $C_{12}$ ,  $C_{13}$ , and  $C_{33}$ , depending on how the bare elastic constants,  $C_{ik}^0$ , were determined. For one set,  $\Delta C_{11} = \Delta C_{12}$  and  $(\Delta C_{13})^2 = \Delta C_{11}\Delta C_{33}$  were assumed (solid lines); for the second set  $\Delta C_{11} = \Delta C_{12} = \Delta C_{13} = \Delta C_{33}$  was assumed (broken lines). In the case of  $C_{13}$  the two curves are almost superimposed.

as the identity representation of the space group of the high symmetry phase. Second, for elastically uniaxial systems (i.e., including quartz) the  $\Delta C_{ik}$  variations are related by:  $\Delta C_{11} = \Delta C_{12}$  and  $(\Delta C_{13})^2 = \Delta C_{11}\Delta C_{33}$  (Axe and Shirane 1970; Höchli 1972; Yamamoto 1974).

Values for the unknown parameters,  $C_{ik}^0$ ,  $A_{ik}$ , and  $K_{ik}$  have been obtained by fitting Equation 37 to the data of Kammer et al. (1948) and Zubov and Firsova (1962) for  $\beta$  quartz (with  $T_c = 840$  K). The two data sets show close agreement over the temperature interval in which they overlap (see Zubov and Firsova 1956). At first, each of  $C_{11}$ ,  $C_{12}$ ,  $C_{13}$ , and  $C_{33}$  was treated separately, producing a range of values of  $K$  between  $-0.57$  ( $K_{13}$ ) and  $-0.77$  ( $K_{12}$ ). These fits did not produce the relationships  $K_{11} = K_{12}$ ,  $A_{11} = A_{12}$ ,  $2K_{13} = K_{11} + K_{33}$ ,  $A_{13}^2 = A_{11}A_{33}$ , expected on the basis of symmetry, however. The variations of  $C_{11}$ ,  $C_{12}$ ,  $C_{13}$ , and  $C_{33}$  are in fact almost parallel, which implies that their  $\Delta C_{ik}$  variations are virtually the same. A fit to the average values  $[(C_{11} + C_{12} + C_{13} + C_{33})/4]$  was therefore performed, yielding  $A = -201.0$  GPa and  $K = -0.65$ . The individual elastic constants were then refit with these two parameters held constant, allowing values

for the bare elastic constants to be determined (listed in Table 3). The value of  $C_{66}^0$  obtained from  $C_{66}^0 = \frac{1}{2}(C_{11}^0 - C_{12}^0)$  was 50.8 GPa, which is in close agreement with the observed variation of  $C_{66}$  shown in Figure 9.  $C_{44}^0 = 37.0$  GPa was selected as an intermediate value between the limits observed for  $C_{44}$  in  $\beta$  quartz. The elastic constant variations above  $T = T_{tr}$  using these parameters are all shown as solid lines in Figure 9.

As an alternative approach, the values of  $K_{11}$  and  $A_{11}$  obtained by fitting the  $C_{11}$  data alone were used in a fit to the  $C_{12}$  data with  $C_{12}^0$  as the only variable parameter, which ensured  $\Delta C_{11} = \Delta C_{12}$  as required by symmetry. Values of  $K_{33}$  and  $A_{33}$  from fitting  $C_{33}$  data alone were then combined with  $K_{11}$  and  $A_{11}$  to give  $K_{13}$  and  $A_{13}$ . These were used to fit the data for  $C_{13}$  and extract a value for  $C_{13}^0$ . This procedure ensured that the relationship  $(\Delta C_{13})^2 = \Delta C_{11}\Delta C_{33}$  was also followed. The resulting parameter values are listed in Table 3, and the fits are shown as broken lines in Figure 9.

The two sets of bare elastic constants were carried through to the calculation of elastic constants for  $\alpha$  quartz. As shown in the next section, they lead to slightly

**TABLE 3.** Values for the coefficients in Equation 8, as used to calculate the elastic constant variations associated with the  $\alpha \leftrightarrow \beta$  transition in quartz

$\Delta C_{11} = \Delta C_{12}, (\Delta C_{13})^2 = \Delta C_{11}\Delta C_{33}$	$\Delta C_{11} = \Delta C_{12} = \Delta C_{13} = \Delta C_{33}$	
4875	$b$ (J/mol)	4634
17218	$c$ (J/mol)	17002
1654	$d$ (J/mol)	1599
3.52	$\lambda_1$ (GPa)	3.38
2.99	$\lambda_3$ (GPa)	2.97
11.9	$\lambda_4$ (GPa)	11.9
29.0	$\lambda_5$ (GPa)	29.0
-6.18	$\lambda_6$ (GPa)	-6.18
1.18	$\lambda_7$ (GPa)	1.13
1.17	$\lambda_8$ (GPa)	1.17
-11.1	$\lambda_9$ (GPa)	-11.1
142.0	$C_{11}^0$ (GPa)	138.3
40.5	$C_{12}^0$ (GPa)	36.8
55.1	$C_{13}^0$ (GPa)	54.0
129.1	$C_{33}^0$ (GPa)	131.2
37.0	$C_{44}^0$ (GPa)	37.0
50.8	$C_{66}^0$ (GPa)	50.8
-0.63	$K_{11} = K_{12}$	-0.65
-0.61	$K_{13}$	-0.65
-0.60	$K_{33}$	-0.65
-232.0	$A_{11} = A_{12}$	-200.9
-190.5	$A_{13}$	-200.9
-149.0	$A_{33}$	-200.9

Notes:  $T_{tr} = 847$  K,  $T_c = 840$  K,  $Q_0 = 0.377$ ,  $a = 9.8$  J/(mol·K),  $b^* = -1931$  J/mol,  $c^* = 10\,190$  J/mol,  $d^* = 0$ .

different values for the strain-order parameter coupling coefficients but do not substantially influence the form of the elastic constant variations. The raw  $C_{ik}$  data of  $\beta$  quartz appear to be consistent with almost isotropic behavior with respect to (non-critical) fluctuations as  $T \rightarrow T_{tr}$ . It is not necessarily the case that the bare elastic constants should be independent of temperature, but given that  $C_{66}$  and  $C_{44}$  vary very little and the lattice parameters of  $\beta$  quartz are approximately constant, any temperature dependence for the  $C_{ik}^0$  values must be small.

Not surprisingly, these fits produce values for the coefficients that are similar to the values given by Höchli (1972) for the same set of experimental data. Axe and Shirane (1970) also analyzed the softening at  $T > T_{tr}$ , but assumed  $K = -1$ , which gives a fit that is not as good.

#### ELASTIC CONSTANT VARIATIONS AT $T < T_{tr}$

To calculate the elastic constants of  $\alpha$  quartz using the equations given in Table 1, it is necessary to have numerical values for all the coefficients in Equation 8. Values of  $C_{ik}^0$  extracted from the elastic properties of  $\beta$  quartz were substituted into Equations 9 and 10. These equations were then matched with the experimental relationships between  $e_i$  and  $Q$  (Eq. 26) to obtain the values for  $\lambda_1$ ,  $\lambda_3$ ,  $\lambda_7$ , and  $\lambda_8$ . The results are listed in Table 3 for the two alternative sets of  $C_{ik}^0$  values. As before, the equilibrium values of  $Q$  were calculated for  $T_{tr} = 847$  K and  $T_c = 840$  K. Both  $C_{44} - C_{44}^0$  and  $C_{66} - C_{66}^0$  are expected to vary linearly with  $Q^2$ , and the experimental data are consistent with this (Bachheimer and Dolino 1975; Dolino and Bachheimer 1982). The linear least-squares fits shown in Figure 10a yielded  $\lambda_4 = 11.9$  GPa,  $\lambda_6 = -6.18$

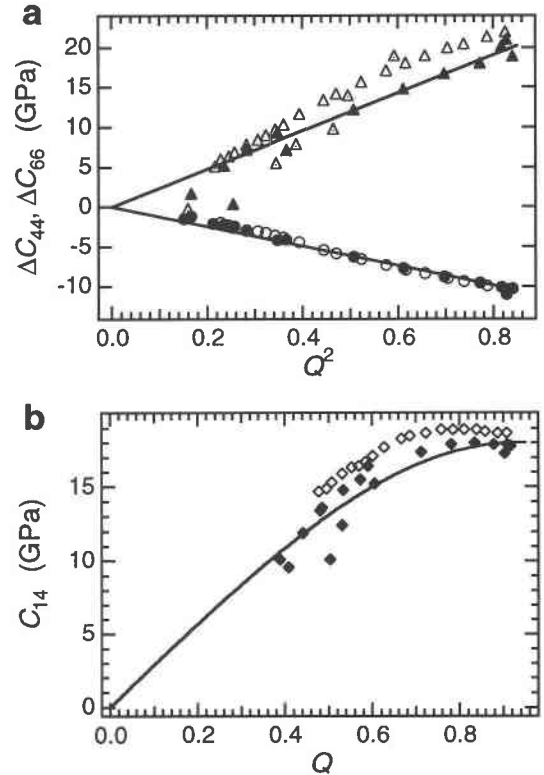


**FIGURE 10.** Relationships between  $C_{44}$ ,  $C_{66}$ ,  $C_{14}$ , and  $Q$  (for  $T_{tr} = 847$  K,  $T_c = 840$  K). (a) The differences  $\Delta C_{44} = C_{44} - C_{44}^0$  (triangles) and  $\Delta C_{66} = C_{66} - C_{66}^0$  (circles) are linear functions of  $Q^2$ . (b) The variation of  $C_{14}$  may be approximated by a curve of the form  $AQ + BQ^3$ . Straight lines and curves are fits to the data represented by filled symbols (from Atanasoff and Hart 1941; Zubov and Firsova 1962; Höchli 1970). Open symbols are data of Ohno (1995); open triangles containing a dot are data of Unoki et al. (1984).

GPa.  $C_{14}$  is expected to vary linearly with  $Q$  but does so only over a limited temperature range below  $T_{tr}$  (Höchli 1970; Höchli and Scott 1971; Bachheimer and Dolino 1975; Dolino and Bachheimer 1982; Ohno 1995). To provide an approximate representation of the evolution of  $C_{14}$ , the next higher order coupling term permitted by symmetry was added to Equation 8. This gives an expected dependence of  $C_{14}$  on  $Q$  of the form  $C_{14} = \lambda_5 Q + \lambda_9 Q^3$  (Table 1), and the fit shown in Figure 10b yielded values of  $\lambda_5 = 29.0$  GPa and  $\lambda_9 = -11.1$  GPa.

Equation 21 provides the most convenient expression for the inverse susceptibility,  $\chi^{-1}$ , as a function of  $Q$ . To use this form it is necessary to have calculated values for the unnormalized Landau coefficients,  $b$ ,  $c$ , and  $d$ . These are readily determined using Equations 11–13; two sets of values corresponding to the two sets of  $\lambda$  and  $C_{ik}^0$  values are given in Table 3. Conversion of units between GPa, the standard units for elastic constants, and J/mol, for the inverse susceptibility and the excess energies, depends on the molar volume of the reference state. This reference state is assumed to have a constant volume and

constant values of  $C_{ik}^0$ , which is not unreasonable given the small thermal expansion observed above  $T_{ir}$ . The unit-cell volume of  $\beta$  quartz has been taken as  $118.1 \text{ \AA}^3$  at 847 K, corresponding to a molar volume of  $2.37 \text{ m}^3/\text{mol}$ ; 1 GPa is thus equivalent to  $2.37 \times 10^4 \text{ J/mol}$ . Values of the equilibrium susceptibility, from Equation 21, were first calculated in joules per mole and converted to gigapascals for substitution into the equations for  $C_{11}$ ,  $C_{12}$ ,  $C_{13}$ , and  $C_{33}$ .

The calculated variations of each elastic constant in  $\alpha$  quartz are compared with experimental observations in Figure 9.  $C_{44}$ ,  $C_{66}$ , and  $C_{14}$  are merely fits to the experimental values, and the quality of fit does not represent a stringent test of the thermodynamic model. On the other hand, the calculated values of  $C_{11}$ ,  $C_{12}$ ,  $C_{13}$ , and  $C_{33}$  are based on fits to experimental data that are entirely independent of the measured elastic constants below  $T_{ir}$ . For  $C_{11}$  and  $C_{12}$ , the match is within reasonable experimental uncertainty and is perhaps marginally better for the set of parameters derived from constraining  $\Delta C_{11} = \Delta C_{12}$  and  $(\Delta C_{13})^2 = \Delta C_{11} \Delta C_{33}$  in  $\beta$  quartz (solid lines). Although the calculated variations of  $C_{13}$  and  $C_{33}$  have the general form of the observed variations, they do not match quantitatively. The choice of bare elastic constants can influence the calculated variations to a limited extent but not enough to explain the discrepancy. All the elastic constants display a small discontinuity at  $T = T_{ir}$ .

The Landau expansion should yield isothermal values of the elastic constants even though ultrasonic (i.e., adiabatic) data were used to derive values for the bare elastic constants,  $C_{ik}^0$ . This assertion is based on the observation that the thermal expansion coefficients of  $\beta$  quartz, which appear in the equation relating isothermal and adiabatic elastic properties (Rehwal 1973; Nye 1985), are small. Immediately below the transition point some divergence between isothermal and adiabatic values is expected (Coe and Paterson 1969; Dolino and Bachheimer 1982). Such a divergence is not evident in Figure 9, however, perhaps because of the first-order character of the transition, which means that the transition occurs before the thermal expansion coefficients become really large.

### ENERGETICS OF THE $\alpha \leftrightarrow \beta$ TRANSITION

Variations of the total excess free energy, enthalpy, and entropy of the  $\alpha \leftrightarrow \beta$  transition (Eqs. 1, 5, and 6, with values of the coefficients given in Table 3) are shown in Figure 11. Different contributions to the free energy can be compared by rewriting Equation 8 as:

$$G = G_Q + G_{\text{coupling}} + G_{\text{elastic}} \quad (38)$$

where  $G_Q$  is the excess energy associated with the driving order parameter alone,  $G_{\text{coupling}}$  is the total energy associated with coupling between  $Q$  and the spontaneous strain, and  $G_{\text{elastic}}$  is the elastic energy,  $\frac{1}{2} \sum_{ik} C_{ik}^0 e_i e_k$ . For  $T = \frac{1}{2} T_{ir} = 424 \text{ K}$  as an example, the equilibrium value of  $Q$  is 0.857. Out of a total excess energy of  $-1085 \text{ J/mol}$  at this temperature, and using the set of coefficients derived from assuming  $\Delta C_{11} = \Delta C_{12}$ ,  $(\Delta C_{13})^2 = \Delta C_{11} \Delta C_{33}$  in  $\beta$

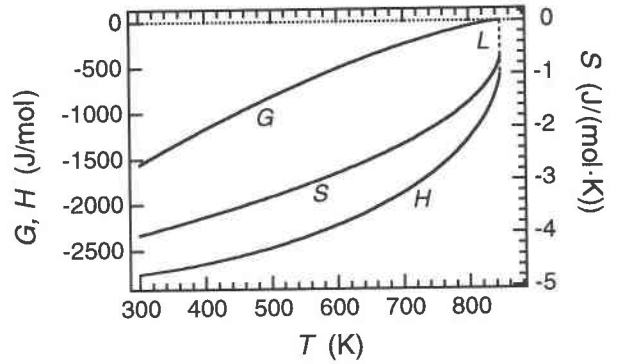
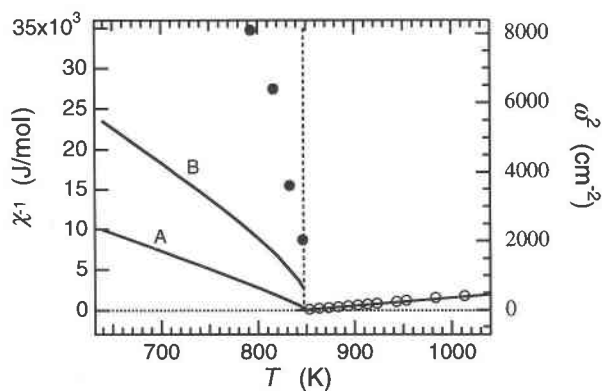


FIGURE 11. Excess free energy ( $G$ ), enthalpy ( $H$ ), and entropy ( $S$ ) associated with the  $\alpha \leftrightarrow \beta$  transition (from Eqs. 1, 5, and 6, with values of the coefficients given in Table 3). The latent heat,  $L$  (broken line), is  $-590 \text{ J/mol}$ .

quartz, the separate energy contributions are  $G_Q = 358 \text{ J/mol}$ ,  $G_{\text{elastic}} = 1442 \text{ J/mol}$ , and  $G_{\text{coupling}} = -2885 \text{ J/mol}$ . The stabilization of  $\alpha$  quartz with respect to  $\beta$  quartz is overwhelmingly dominated by the energy associated with coupling of the order parameter with the spontaneous strain. This coupling can also account for the first-order character of the transition. The renormalized fourth-order coefficient,  $b^*$ , is  $-1931 \text{ J/mol}$ , but its unrenormalized value is  $\sim 4900 \text{ J/mol}$ . The fourth-order term should thus be positive and the phase transition thermodynamically continuous in a clamped crystal with zero strain.

The soft zone center ( $B_1$ ) optic mode observed by Axe and Shirane (1970), and Dolino et al. (1992) is generally regarded as providing the driving mechanism for the transition (as reviewed recently by Heaney 1994; Dolino and Vallade 1994). If this is correct, it should be possible to link the energetics of the transition to the soft mode by means of the susceptibility. The frequency of a classical soft mode at  $T > T_{ir}$  is expected to depend explicitly on the order parameter susceptibility as  $\omega^2 \propto \chi^{-1}$  (see, for example, Bruce and Cowley 1981, or Dove 1993). Below the transition point the same dependence is also expected, but when coupling with a strain occurs, there may be some doubt as to whether the soft mode frequency depends on the renormalized or unrenormalized susceptibility. The present analysis permits comparison of both with the observed frequency. Data from Tezuka et al. (1991) for the soft mode in  $\beta$  quartz are shown in Figure 12. The inverse susceptibility at  $T > T_{ir}$  is given by  $a(T - T_c)$  and has been plotted on the same figure (for  $a = 9.8 \text{ J/mol}$  and  $T_c = 840 \text{ K}$ ). Vertical axes, in units of inverse centimeters squared and joules per mole were adjusted so that the  $\omega^2$  and  $\chi^{-1}$  variations coincide. Experimental data from Höchli and Scott (1971) for the soft mode frequency below  $T_{ir}$  and two sets of variations for  $\chi^{-1}$  are also shown on the same relative scale. If changes in strain can occur on the same time scale as changes in  $Q$ , the susceptibility of the soft mode is derived from the fully renormalized Landau expansion (Eq. 1) as:



**FIGURE 12.** Comparison between experimental data for the frequency of the soft mode and the calculated susceptibility from a Landau free energy expansion. A relationship of the form  $\omega^2 \propto \chi^{-1}$  is expected. The axes for  $\omega^2$  (right) and  $\chi^{-1}$  (left) have been adjusted so that, above  $T_{tr}$ , the experimental data for  $\omega^2$  (open circles, from Tezuka et al. 1991) are superimposed on the calculated variation of  $\chi^{-1}$  (solid line). Below  $T_{tr}$ , experimental data for  $\omega^2$  are shown as filled circles (from Höchli and Scott 1971). Curve A is the fully renormalized susceptibility (Eq. 39) and curve B is the unrenormalized susceptibility (Eq. 21). (Note that the mismatch below  $T_{tr}$  could be reduced by choosing an alternative scaling between  $\omega^2$  and  $\chi^{-1}$  at  $T > T_{tr}$ .)

$$\chi^{-1} = \left( \frac{\partial^2 G}{\partial Q^2} \right) = a(T - T_c) + 3b*Q^2 + 5c*Q^4. \quad (39)$$

This solution is curve A in Figure 12. If the response time of the structure to changes in  $Q$  is much shorter than the response time to changes in strain, the relevant susceptibility is given by Equation 21. Curve B in Figure 12 shows the calculated variation for the set of coefficients derived from assuming  $\Delta C_{11} = \Delta C_{12}$  and  $(\Delta C_{13})^2 = \Delta C_{11}\Delta C_{33}$  in  $\beta$  quartz. In this case the role of strain is only to renormalize the shape of the potential well that determines the soft mode frequency. It more nearly reproduces the steep recovery of  $\omega^2$  below  $T_{tr}$ , but neither solution matches the observed soft-mode frequency changes. The mismatch may indicate that either the soft mode is not the only driving mechanism for the transition or the frequency evolution of the  $B_1$  optic mode is substantially modified by coupling with other modes. For example, strong coupling occurs between low frequency modes at the  $\Gamma$  point (zone center), at the zone boundary M point, and along the  $\Gamma$ -M direction (Dolino and Vallade 1994 and references therein). If the numerical relationship between  $\chi^{-1}$  and  $\omega^2$  at  $T > T_{tr}$  were rescaled by choosing a smaller value of the  $a$  coefficient, for example, it might be possible to obtain a closer match between  $\chi^{-1}$  and  $\omega^2$  at  $T < T_{tr}$ . This model would imply that there are contributions to the entropy other than those from the soft optic mode. Finally, note that because of the steep recovery of the soft mode below  $T_{tr}$  it is unlikely that thermal fluctuations of the type responsible for the elastic softening in  $\beta$  quartz have a significant role in the  $\alpha$  quartz structure.

## GEOMETRICAL ASPECTS OF THE TRANSITION MECHANISM

The  $\alpha \leftrightarrow \beta$  transition has been described in purely geometrical terms as rotations of  $\text{SiO}_4$  tetrahedra about the  $\langle 100 \rangle$  axes (Höchli and Scott 1971; Megaw 1973; Grimm and Dörner 1975; and many subsequent authors). The rotation angle,  $\phi$ , is generally considered to be the microscopic order parameter;  $\phi = 0$  in  $\beta$  quartz and  $\phi \approx 16.3^\circ$  in  $\alpha$  quartz at room temperature. These rotations are then held to be responsible for the macroscopic lattice strains. In this context, Grimm and Dörner (1975) separated three effects. First, rotation of rigid tetrahedra produces a direct reduction of the lattice parameters of the framework. Second, the rotations cause a reduction in the Si-O-Si bond angle, and this reduction is correlated with an increase in the Si-O bond lengths. Third, the tetrahedra are subject to a shearing deformation that gives a net increase in the direction of the  $c$  axis. All three processes are interdependent and are due to a change in the nature of the Si-O bonds with temperature. In principle, non-linearities in the macroscopic strains must reflect some non-linearities in these microscopic distortions.

Rotations of rigid tetrahedra only produce macroscopic spontaneous strains that scale closely with  $\phi^2$  (Grimm and Dörner 1975). The standard argument for this is simple. Rotation through an angle  $\phi$  produces changes in the  $a$  and  $c$  parameters that vary with  $\cos \phi$  (Taylor 1972; Megaw 1973). Expanding  $\cos \phi$  gives:

$$\cos \phi = 1 - \frac{1}{2}\phi^2 + \frac{1}{24}\phi^4 - \dots \quad (40)$$

For  $\phi = 0.28$  rad ( $\sim 16^\circ$ ), the fourth order term is only  $\sim 1\%$  ( $\sim 0.0003$ ) of the second order term ( $\sim 0.039$ ). Even for such large rotation angles, therefore, the higher order contribution to the change in lattice parameters is negligibly small.

There is a well-recognized correlation between decreasing Si-O-Si bond angles and increasing Si-O bond lengths in framework silicates (Hill and Gibbs 1979). The mean Si-O bond lengths,  $d_{\text{Si-O}}$ , appear to vary linearly with  $\phi^2$  (Fig. 13), though the correlation remains empirical (data from Kihara 1990, both for  $d_{\text{Si-O}}$  and for  $\phi$  calculated using the equation given by Grimm and Dörner 1975; Dolino and Bachheimer 1982; Lager et al. 1982). This microscopic contribution to the macroscopic strain is a more or less isotropic expansion of the whole framework.

The effects of shearing are evident in the  $c/a$  ratio. As shown by Smith (1963), this ratio must be less than or equal to 1.0981 if the  $\text{SiO}_4$  tetrahedra in quartz are perfectly regular. It is expected to decrease as the Si-O-Si angle decreases and  $\phi$  increases but the reverse is actually observed (Lager et al. 1982; Fig. 14a). There seems little doubt that the tetrahedra are significantly deformed (Smith 1963; Megaw 1973; Grimm and Dörner 1975; Lager et al. 1982; Barron et al. 1982). The contribution of this deformation to the macroscopic strain can be esti-

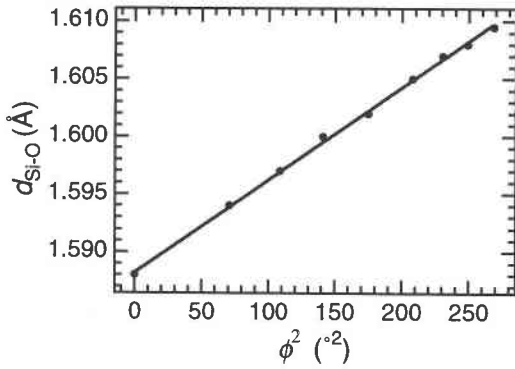


**FIGURE 13.** Linear variation of the mean Si-O bond length,  $d_{\text{Si-O}}$ , with the square of the rotation angle,  $\phi$ , of tetrahedra about the  $\langle 100 \rangle$  axes. Data from Kihara (1990), using the Equation of Grimm and Dörner (1975) to calculate  $\phi$  from structural data.

ated as follows. For  $\phi \approx 16^\circ$ , rotations of rigid tetrahedra would give strains of  $e_{1,\text{rot}} = -0.025$  and  $e_{3,\text{rot}} = -0.040$  (using the equations of Grimm and Dörner 1975, for  $a$  and  $c$  as functions of  $\phi$ ). At the same time, the mean Si-O bond distance would increase by  $\sim 1.4\%$  (from Fig. 13). Treating this as a more or less isotropic effect in relation to the whole framework yields contributions to both strains of  $e_{1,\text{d}} \approx e_{3,\text{d}} \approx 0.014$ . The observed room temperature values of  $e_1$  and  $e_3$  are  $-0.016$  and  $-0.010$ , respectively, which leaves contributions from shearing of  $e_{1,\text{sh}} \approx -0.005$  and  $e_{3,\text{sh}} \approx +0.016$  ( $e_1 = e_{1,\text{rot}} + e_{1,\text{d}} + e_{1,\text{sh}}$ , etc.). The contribution of the shearing component to the volume strain,  $2e_{1,\text{sh}} + e_{3,\text{sh}} = 0.006$ , is small relative to the total volume strain of  $2e_1 + e_3 = -0.042$ , indicating that this part of the total deformation is indeed close to pure shear.

From this semi-quantitative analysis it is clear that the macroscopic consequences of the three geometrical effects discussed by Grimm and Dörner have similar magnitudes. By a process of elimination, the non-linear strain behavior might be attributed to the shearing of the tetrahedra. The effects of such shearing on a macroscopic scale can be examined further by focussing on the variation of  $c/a$  with temperature, which closely resembles the typical evolution of “excess” properties caused by a phase transition (Fig. 14a). Accordingly, an effective shear strain  $\Delta(c/a)$  may be defined as:

$$\Delta(c/a) = \frac{(c/a) - (c/a)_0}{(c/a)_0} \quad (41)$$

where  $(c/a)_0$  is the ratio for  $\beta$  quartz extrapolated to  $T < T_{\text{tr}}$ . With the exception of four data points from temperatures between  $\sim 815$  and  $\sim 842$  K and data from below room temperature (the latter showing the influence of order parameter saturation), this effective shear strain appears to vary linearly with  $Q^2$  for  $T_{\text{tr}} = 847$  K,  $T_{\text{c}} = 840$  K (Fig. 14b).

Such a shear parameter is not a properly constituted strain in the thermodynamic sense. In particular, this pa-

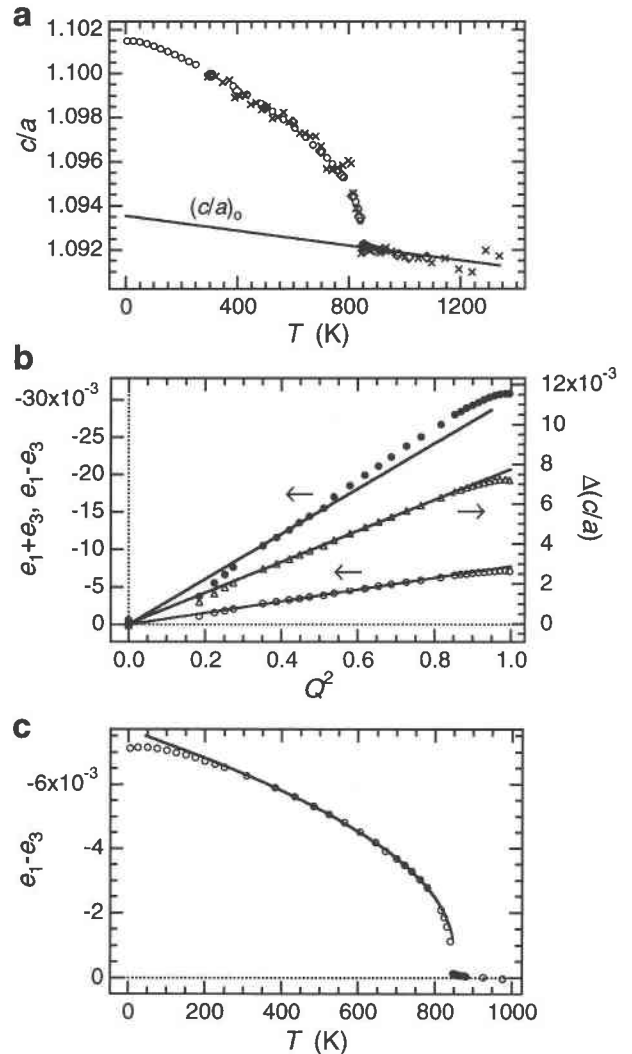


**FIGURE 14.** (a) The  $c/a$  ratio for  $\alpha$  quartz should be less than that of  $\beta$  quartz if the transition is due to rotations of tetrahedra that remain rigid. Open circles = neutron data; crosses = X-ray data. Data from Kihara (1990) are also shown for comparison (open diamonds). The observed increase with falling temperature indicates that the tetrahedra become progressively deformed with falling temperature. The ratio  $c/a$  appears to behave in a similar manner to other excess properties and can be converted into an effective shear strain,  $\Delta(c/a)$ , using Equation 41. (b) For  $0.3 < Q^2 < 0.9$ ,  $\Delta(c/a)$  (open triangles) scales linearly with  $Q^2$  (for  $T_{\text{tr}} = 847$  K,  $T_{\text{c}} = 840$  K). The data for  $e_1 - e_3$  (open circles) show a similar linear variation, but the data for  $e_1 + e_3$  (filled circles) do not. (c) The fit to a Landau solution for a first order transition (solid line) for  $e_1 - e_3$  between 300 and 800 K gives  $T_{\text{tr}} - T_{\text{c}} = 8.4$  K (for  $T_{\text{tr}} = 847$  K).

parameter is not related in a simple way to any eigenvector of the elastic constant matrix of  $\beta$  quartz. For a more rigorous formal analysis, reference to the eigenvalues and eigenvectors of the elastic constant matrix of materials with crystallographic point group 622 is required. These are listed in Table 4 (examples of this type of symmetry

**TABLE 4.** Eigenvalues and eigenvectors of the elastic constant matrix for point group 622 (Laue class 6/*mmm*)

Irreducible representation	Eigenvalue	Eigenvector	Symmetry-adapted spontaneous strain
$A_1$	$\frac{1}{2}[(C_{11} + C_{12} + C_{33}) - [(C_{11} + C_{12} - C_{33})^2 + 8C_{44}^2]^{1/2}]$	$(\alpha, \alpha, \beta, 0, 0, 0)^*$	$e_1 + e_2; e_3$
$A_1$	$\frac{1}{2}[(C_{11} + C_{12} + C_{33}) + [(C_{11} + C_{12} - C_{33})^2 + 8C_{44}^2]^{1/2}]$	$(\alpha', \alpha', \beta', 0, 0, 0)^*$	$e_1 + e_2; e_3$
$E_1$	$\begin{cases} C_{44} \\ C_{44} \end{cases}$	$\begin{matrix} A(0, 0, 0, 1, 0, 0)^* \\ B(0, 0, 0, 0, 1, 0) \end{matrix}$	$\begin{matrix} e_4 \\ e_5 \end{matrix}$
$E_2$	$\begin{cases} (C_{11} - C_{12}) \\ (2)C_{66}\dagger \end{cases}$	$\begin{matrix} D\left(\frac{1}{\sqrt{2}}, -\frac{1}{\sqrt{2}}, 0, 0, 0, 0\right)^* \\ E(0, 0, 0, 0, 0, 1) \end{matrix}$	$\begin{matrix} \frac{1}{\sqrt{2}}(e_1 - e_2) \\ \left(\frac{1}{\sqrt{2}}\right)e_6\dagger \end{matrix}$

\*  $2\alpha^2 + \beta^2 = 2\alpha'^2 + \beta'^2 = 1, 2\alpha\alpha' + \beta\beta' = 0, A^2 + B^2 = D^2 + E^2 = 1$ .  
 † The  $E_2$  eigenvalues are required to be identical but, as an artifact of the convention used to reduce  $C_{ijk}$  to  $C_{ik}$ , come out as  $(C_{11} - C_{12})$  and  $C_{66}$ . Because  $C_{66} = \frac{1}{2}(C_{11} - C_{12})$  in hexagonal systems, a factor of two must be applied to  $C_{66}$  and a corresponding factor of  $1/\sqrt{2}$  to  $e_6$  (shown in brackets) to give the correct degeneracies.

analysis are given elsewhere in the literature; see Boccara 1968; McLellan 1973; Cowley 1976; Bulou 1992; Bulou et al. 1992; Carpenter and Salje, unpublished manuscript). The important point is that there are two degenerate eigenvalues associated with the identity representation,  $A_1$ . The spontaneous strains associated with these are derived from the eigenvectors and correspond to combinations of strains parallel and perpendicular to the  $c$  axis in different proportions. One must have contributions to both  $(e_1 + e_2)$  and  $e_3$  with the same sign, whereas the second must have contributions to  $(e_1 + e_2)$  and  $e_3$  with opposite sign (also see McLellan 1973). It is tempting to associate the first,  $\epsilon_{rot}$ , with strains arising from the tetrahedral rotations and the variations in mean Si-O bond lengths and the second,  $\epsilon_{sh}$ , with shearing of the tetrahedra (lengthening parallel to  $c$  and shortening perpendicular to  $c$ ). They are orthogonal by definition, and are thus able to couple independently with the driving order parameter. If the rotation angle  $\phi$  is not a linear function of  $Q$ , the overall microscopic and macroscopic strain behavior could be described by:

$$\epsilon_{rot} = AQ^2 + BQ^4 \propto \phi^2 \quad (42)$$

$$\epsilon_{sh} = C\phi^2 + D\phi^4 \propto Q^2 \quad (43)$$

where  $A$ ,  $B$ ,  $C$ , and  $D$  are effective coupling constants.

It is not straightforward to obtain values for the parameters  $\alpha$ ,  $\alpha'$ ,  $\beta$ ,  $\beta'$  in the eigenvector expressions, but a combination of strains that can be used as an approximation for the macroscopic shearing is the difference  $e_1 - e_3$ . This difference also varies almost linearly with  $Q^2$  between  $\sim 300$  and  $\sim 800$  K, in marked contrast with the sum  $e_1 + e_3$  (Fig. 14b). If  $e_1 - e_3$  scales with  $Q^2$ , the same procedure as used for analyzing the temperature dependence of the volume strain can be applied using Equations 2 and 25. The resulting fit to data for  $e_1 - e_3$  in the range 300–800 K is shown in Figure 14c, with  $T_u - T_c = 8.4$  K (for  $T_u = 847$  K). Over many hundreds of degrees the evolution of this shearing parameter is thus al-

most indistinguishable from the second harmonic generation (SHG) parameter of Bachheimer and Dolino (1975).

Taken at face value, the macroscopic shearing of the  $\alpha$  quartz structure appears to vary linearly with  $Q^2$ , the individual strains  $e_1$  and  $e_3$  vary with  $AQ^2 + BQ^4$ , but contributions from rotations of rigid tetrahedra and increased mean Si-O bond lengths vary linearly with  $\phi^2$ . Because the volume strain is given by  $V_s = e_1 + e_2 + e_3$ , to a good approximation, the non-linear coupling with  $Q^2$  appears in the excess volume associated with the transition. There is, therefore, some question as to the relationship between the macroscopic order parameter and the tetrahedral rotations. Values of  $\phi$  quoted in the literature have been derived from the structural study of Young (1962) (e.g., Grimm and Dorner 1975; Crane and Bergman 1976; Dolino and Bachheimer 1982; Dolino et al. 1983; Dolino 1988, 1990). They are plotted against  $Q$  (for  $T_u = 847$  K,  $T_c = 840$  K) in Figure 15, as are values extracted from the refinements of Kihara (1990) and from SHG data by Crane and Bergman (1976). The data from Young (1962) show a linear correlation, with some scatter, whereas the data from Kihara (1990) are more consistent with a non-linear correlation. Further structural studies may be needed to test this possibility.

In the lattice parameters obtained by neutron diffraction and in the strain parameters derived from them there is some suggestion of a change in trend at  $\sim 650$  K (at  $Q^2 \approx 0.53$  in Figs. 4 and 14b, for example). The variation of  $c/a$  with unit-cell volume has been taken in the past as an indicator of how uniformly the thermal expansion mechanisms of  $\alpha$  quartz operate over a wider temperature interval (Lager et al. 1982). The neutron data show an almost linear relationship from the transition temperature down to  $\sim 300$  K (Fig. 16) but there is also a hint of a break in slope at  $c/a \approx 1.0968$  ( $\sim 650$  K). The changes are small and require further investigation but could signal some change in the relationship between shearing and rotations of the tetrahedra. As  $T$  increases above  $T_u$ ,  $c/a$



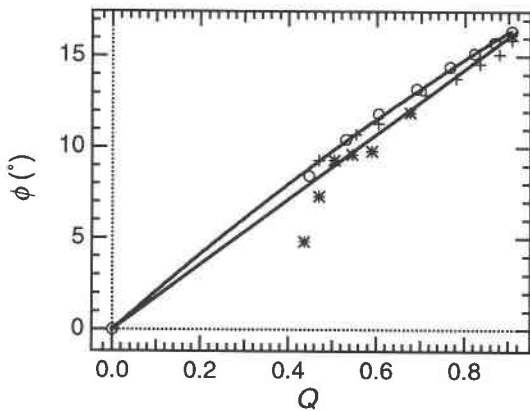


FIGURE 15. Relationships between the rotation angle  $\phi$  and the macroscopic order parameter,  $Q$  (for  $T_{tr} = 847$  K,  $T_c = 840$  K). Open circles: values of  $\phi$  extracted from structure refinements of Kihara (1990). Stars = data of Young (1962) in Dolino (1990). Crosses = values of  $\phi$  calculated from SHG data by Crane and Bergman (1976). The straight line is a guide to the eye through the relatively scattered data from Young (1962). The curve is a fit of an equation with the form  $\phi = AQ + BQ^2$  to the data of Kihara (1990).

decreases at constant volume, and there is also a different trend in the low-temperature region of order parameter saturation.

### DISCUSSION

As found by previous authors, the Landau 2-4-6 potential provides a basis for describing the changes in physical properties that accompany the  $\alpha \leftrightarrow \beta$  transition in quartz. The new determination of strain behavior and analysis of both elastic constants and heat capacity data confirm that this potential can be used to link different physical effects associated with the transition, but they also highlight some discrepancies. The internally consistent set of values determined for the three temperatures,  $T_c$ ,  $T_{tr}$ , and  $T_i$ , from studies of the soft mode, the phase transition temperatures, SHG and  $C_p$  data, in principle place tight constraints on the evolution of the macroscopic order parameter,  $Q$ . The two sets of lattice parameters presented here were obtained by entirely independent methods from the same original quartz sample. They are indistinguishable within reasonable experimental uncertainty and overlap with other data from the recent literature (e.g., Fig. 4 and Fig. 14a). The evolution of the strain parameters is also well-constrained. What appears to be unusual is the nature of coupling between the strains and the driving order parameter. The only other materials known to us to develop strains that do not correlate simply with the lowest order function of  $Q$  permitted by symmetry are albite and  $\text{BiVO}_4$  (Salje et al. 1985; David and Wood 1983; Carpenter et al., unpublished manuscript). However, it is not only the strain coupling that behaves anomalously. Both the elastic constant  $C_{14}$  (data in Fig. 10b) and the piezoelectric coefficient  $d_{11}$  (data of Cook

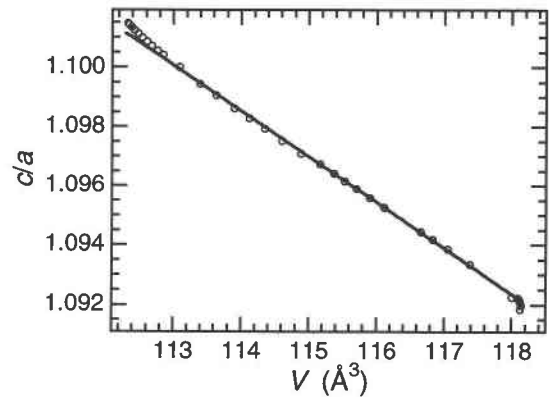


FIGURE 16. Neutron diffraction data showing that the  $c/a$  ratio varies smoothly with unit-cell volume for both  $\alpha$  and  $\beta$  quartz. The straight line was fit to the data points with values of  $V$  in the range  $\sim 115$ – $116.2 \text{ \AA}^3$ , corresponding to the temperature interval  $\sim 670$ – $780$  K. It passes through the data points for  $\beta$  quartz close to  $T_{tr}$  ( $V \approx 118 \text{ \AA}^3$ ), but seems to highlight a small change in trend below  $V \approx 115 \text{ \AA}^3$  ( $\sim 650$  K).

and Weissler 1950) show substantial deviations from the linear variation with  $Q$  expected on symmetry grounds (Bachheimer and Dolino 1975; Dolino and Bachheimer 1982).

The quality of fit between the calculated and observed variations of  $C_{11}$ ,  $C_{12}$ ,  $C_{13}$ , and  $C_{33}$  in  $\alpha$  quartz provides a necessary (but not sufficient) test of the form of coupling between  $Q$  and strain in the full Landau expansion (Eq. 8). Extraneous experimental factors in the elasticity measurements do not seem relevant. No systematic difference exists between results from Brillouin scattering or ultrasonic experiments, and the more recent room temperature elastic constant data of Wang et al. (1992) are barely distinguishable from the older data. In this context, close agreement between the observed and calculated variations of  $C_{11}$  and  $C_{12}$  is encouraging. On the other hand, failure to reproduce the variation of  $C_{33}$  below  $\sim 700$  K more precisely than shown in Figure 9 indicates that, although the overall analysis gives a fair representation of the complete strain and elastic behavior, strain parallel to the  $c$  axis has not been accounted for entirely correctly. The model inherent in Equation 8 incorporates the assumptions that only one order parameter is needed to describe the structural evolution of  $\alpha$  quartz with respect to  $\beta$  quartz and that each strain can be described by a single, continuous curve (Fig. 4). The apparent breaks in behavior of the strains at  $\sim 650$  and  $\sim 800$  K signify that these are oversimplifications. One possibility is that the relative contributions of tetrahedral rotations and tetrahedral shear differ in three temperature intervals: 847–800 K, 800–650 K, and 650–300 K. In other words, there is an additional degree of freedom in the system. Alternatively, some different distortion might be initiated at  $\sim 650$  K, in which case the additional strain below this temperature must be accounted for separately. Megaw (1973) has commented on the fact

that the Si atoms seemingly start to move off-center within their tetrahedra near 450 °C (723 K). Finally, just below  $T_{tr}$  the transition could involve a mix of displacive and order-disorder character.

From a purely energetic point of view, the phase transition is driven overwhelmingly by coupling of the order parameter with strain. The overall conclusion is similar to that of Tautz et al. (1991) who considered the importance of volume reduction from the perspective of phonon interactions. For a combination of structural and symmetry reasons, the  $\beta$  quartz structure is unable to reduce its volume with falling temperature. The  $B_1$  soft optic mode effectively provides a mechanism by which to break the symmetry, and once the symmetry is reduced, the  $\alpha$  quartz structure is able to resume a more normal pattern of thermal expansion. The energetic contribution of the soft mode to the transition mechanism is small.

Rather than displaying thermal expansion, the  $\beta$  structure is subject to significant thermal fluctuations. The observed pattern of elastic softening suggests that it behaves as a more or less isotropic medium with respect to these fluctuations. Not only are  $\Delta C_{11}$ ,  $\Delta C_{12}$ ,  $\Delta C_{13}$ , and  $\Delta C_{33}$  very similar (under the assumption of constant  $C_{ik}^0$ ), but also the exponents  $K_{ik}$  have values between  $-0.5$  and  $-1$ . The value of  $K$  is known to be sensitive to the degree of anisotropy of dispersion curves around the reciprocal lattice vector of the soft mode and to the extent of softening along each branch (Axe and Shirane 1970; Pytte 1970, 1971; Höchli 1972; Carpenter and Salje, unpublished manuscript). A value of  $K = -0.5$  is expected if the branches of the soft mode all soften more or less uniformly in three dimensions (Carpenter and Salje, unpublished manuscript). Such a uniform effect is in part borne out by investigations of the lowest frequency acoustic modes. Softening has been observed along  $a^*$  (Boysen et al. 1980; Berge et al. 1986) and plays a crucial role in stabilizing the incommensurate phase just above  $T_{tr}$  (Dolino 1988, 1990; Tautz et al. 1991; Dolino et al. 1992; Vallade et al. 1992; Dolino and Vallade 1994). Calculated dispersion relations indicate that an acoustic branch is also relatively flat along  $c^*$  and softens uniformly as  $T \rightarrow T_{tr}$  (e.g., Kihara 1993). This softening is presumed to occur as a consequence of softening of the soft optic mode. Nearly isotropic behavior is also reflected in the similar values of the coupling constants for the macroscopic strains parallel and perpendicular to the  $c$  axis of  $\alpha$  quartz.

Our understanding of the geometrical and thermodynamic features of the  $\alpha \leftrightarrow \beta$  transition in quartz clearly remains incomplete. The elastic properties give additional insights but to what extent can the transition be regarded as having an elastic origin? The  $B_1$  soft optic mode is associated with the active representation for the transition and provides the mechanism for breaking symmetry. Coupling with strain then gives elastic anomalies associated with the identity representation. McLellan (1973) suggested that one of the  $A_1$  eigenvalues of the elastic constant matrix might extrapolate to zero

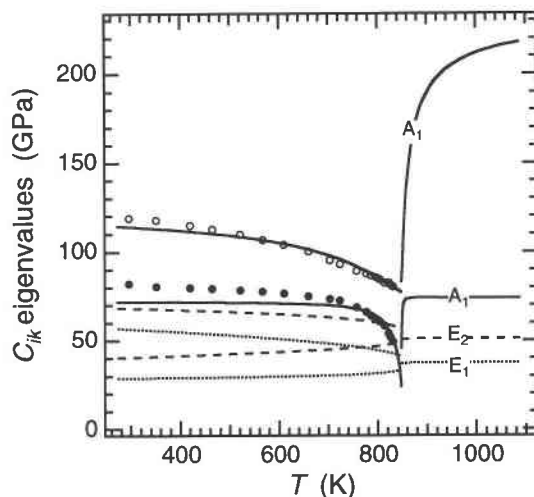


FIGURE 17. Variations of the eigenvalues of the elastic constant matrix for crystals with point group 622 ( $T > T_{tr}$ ) and point group 32 ( $T < T_{tr}$ ). Expressions for the eigenvalues of 622 crystals are given in Table 4. ( $E_1$  is plotted as  $C_{44}$ ;  $E_2$  is plotted as  $C_{66}$ ).  $A_1$  eigenvalues of crystals with 32 symmetry have the same form as those of crystals with 622 symmetry. The smooth curves were determined from the calculated variations shown in Figure 9 (data from solutions derived from assuming  $\Delta C_{11} = \Delta C_{12}$  and  $(\Delta C_{13})^2 = \Delta C_{11}\Delta C_{33}$  in  $\beta$  quartz). Solid lines represent the  $A_1$  eigenvalues; broken and dotted lines represent the other eigenvalues. Each of the  $E_1$  and  $E_2$  eigenvalues of  $\beta$  quartz splits into two in  $\alpha$  quartz. Experimental data points for  $A_1$  eigenvalues are shown below  $T_{tr}$  (data from Ohno 1995). There is reasonable agreement between calculated and experimental data over the complete temperature range for one of the  $A_1$  eigenvalues and close agreement over the range  $T_{tr}$  to  $\sim 750$  K for the other. Neither of the  $A_1$  eigenvalues reaches zero at the transition point.

at the transition point in much the same way that eigenvalues associated with the active representation can evolve at a proper ferroelastic transition (Rehwald 1973; Cowley 1976; Lüthi and Rehwald 1981; Wadhawan 1982; Toledano et al. 1983; Bulou et al. 1992; Carpenter and Salje, unpublished manuscript). Following McLellan (1973), variations in the numerical values of the eigenvalues given in Table 4 (for point group 622) have been calculated using the set of data derived from assuming  $\Delta C_{11} = \Delta C_{12}$ ,  $(\Delta C_{13})^2 = \Delta C_{11}\Delta C_{33}$ . An equivalent set of expressions for point group 32 was used to calculate the eigenvalues of  $\alpha$  quartz. These variations are all shown in Figure 17. Data from Ohno (1995) were used to compute experimental values of the  $A_1$  eigenvalues, for comparison.

Anomalies in the elastic behavior are indeed predominantly associated with the eigenvalues of the  $A_1$  (identity) representation. Above  $T_{tr}$ , one eigenvalue shows the fluctuation induced softening while the other displays a more classical form, being effectively constant. (The small dip close to  $T_{tr}$  of the latter is highly sensitive to the extrapolated values of  $C_{13}^0$  and may or may not be

real). Both show softening as  $T_{tr}$  is approached from below, and the calculated variations match the experimental data down to  $\sim 700$  K (Fig. 17). There is no evidence that either approaches zero in value. In this regard, the elastic behavior is entirely consistent with the behavior of a classical co-elastic material (Salje 1993). On the other hand, the individual elastic constant  $C_{13}$  extrapolates to zero at  $847 \pm 1$  K from  $T > T_{tr}$  (see Fig. 9). By itself, this cannot lead to an elastic instability, but it corresponds to a limiting point beyond which the elastic energy  $\frac{1}{2}C_{13}e_1e_3$  for  $e_1$  and  $e_3$  with the same sign becomes negative, i.e., starting to favor simultaneous contraction parallel and perpendicular to the  $c$  axis. Furthermore, the temperature interval below  $T_{tr}$  over which  $e_1$  and  $e_3$  do not conform to the predicted pattern (Fig. 5) corresponds to the temperature interval over which  $C_{13}$  remains negative in  $\alpha$  quartz. In any macroscopic model of the transition, the elastic properties may not be regarded as driving the transition, but they are certainly associated with most of the energy change.

### ACKNOWLEDGMENTS

Part of this work was completed while B.W. was supported by a grant from the Natural Environment Research Council (GR3/8220'A'), which is gratefully acknowledged. The U.K. Science and Engineering Research Council is also thanked for HRPD beam time at the Rutherford-Appleton Laboratory.

### REFERENCES CITED

- Ackerman, R.J. and Sorrell, C.A. (1974) Thermal expansion and the high-low transformation in quartz: I. High-temperature X-ray studies. *Journal of Applied Crystallography*, 1, 461–467.
- Aleksandrov, K.S. and Flerov, I.N. (1979) Ranges of applicability of thermodynamic theory of structural phase transitions near the tricritical point. *Soviet Physics. Solid State*, 21, 195–200.
- Atanasoff, J.V. and Hart, P.J. (1941) Dynamical determination of the elastic constants and their temperature coefficients for quartz. *Physical Review*, 59, 85–96.
- Atanasoff, J.V. and Kammer, E. (1941) A determination of the  $C_{44}$  elastic constant for beta-quartz. *Physical Review*, 59, 97–99.
- Axe, J.D. and Shirane, G. (1970) Study of the  $\alpha$ - $\beta$  quartz phase transformation by inelastic neutron scattering. *Physical Review*, B1, 342–348.
- Bachheimer, J.P. (1980) An anomaly in the  $\beta$  phase near the  $\alpha$ - $\beta$  transition of quartz. *Journal de Physique Lettres*, 41, L559–L561.
- (1986) Optical rotatory power and depolarisation in the  $\alpha$ -, incommensurate and  $\beta$ -phases of quartz (20 to 600°C). *Journal of Physics C*, 19, 5509–5517.
- Bachheimer, J.P. and Dolino, G. (1975) Measurement of the order parameter of  $\alpha$ -quartz by second-harmonic generation of light. *Physical Review*, B11, 3195–3205.
- (1980) Study of thermal expansion of quartz near the  $\alpha$ - $\beta$  phase transition under uniaxial stress. *Ferroelectrics*, 25, 423–426.
- Banda, E.J.K.B., Craven, R.A., and Parks, R.D. (1975)  $\alpha$ - $\beta$  transition in quartz: classical versus critical behavior. *Solid State Communications*, 17, 11–14.
- Barron, T.H.K., Collins, J.F., Smith, T.W., and White, G.K. (1982) Thermal expansion, Grüneisen functions and static lattice properties of quartz. *Journal of Physics*, C15, 4311–4326.
- Berge, B., Bachheimer, J.P., Dolino, G., and Vallade, M. (1986) Inelastic neutron scattering study of quartz near the incommensurate phase transition. *Ferroelectrics*, 66, 73–84.
- Boccaro, N. (1968) Second-order phase transitions characterized by a deformation of the unit cell. *Annals of Physics*, 47, 40–64.
- Boysen, H., Dorner, B., Frey, F., and Grimm, H. (1980) Dynamic structure determination for two interacting modes at the M-point in  $\alpha$ - and  $\beta$ -quartz by inelastic neutron scattering. *Journal of Physics*, C13, 6127–6146.
- Bruce, A.D. and Cowley, R.A. (1981) *Structural phase transitions*, 326 p. Taylor and Francis, London.
- Bulou, A. (1992) On considering the elastic constant table as the matrix of an operator; consequences in ferroelasticity. *Journal de Physique I*, 2, 1445–1460.
- Bulou, A., Rousseau, M., and Nouet, J. (1992) Ferroelastic phase transitions and related phenomena. *Key Engineering Materials*, 68, 133–186.
- Cao, W. and Barsch, G.R. (1988) Elastic constants of KMnF<sub>3</sub> as functions of temperature and pressure. *Physical Review*, B38, 7947–7958.
- Carpenter, M.A. (1992) Thermodynamics of phase transitions in minerals: a macroscopic approach. In G.D. Price and N.L. Ross, Eds., *The stability of minerals*, p. 172–215. Chapman and Hall, London.
- Coe, R.S. and Paterson, M.S. (1969) The  $\alpha$ - $\beta$  inversion in quartz: a coherent phase transition under nonhydrostatic stress. *Journal of Geophysical Research*, 74, 4921–4948.
- Cook, R.K. and Weissler, P.G. (1950) Piezoelectric constants of Alpha and Beta-quartz at various temperatures. *Physical Review*, 80, 712–716.
- Cowley, R.A. (1976) Acoustic phonon instabilities and structural phase transitions. *Physical Review*, B13, 4877–4885.
- Crane, G.R. and Bergman, J.G. (1976) Structural mechanics from nonlinear optics—the  $\alpha$  to  $\beta$  phase transition in quartz. *Journal of Applied Crystallography*, 9, 476–480.
- Cummins, H.Z. (1979) Brillouin scattering spectroscopy of ferroelectric and ferroelastic phase transitions. *Philosophical Transactions of the Royal Society of London A*, 293, 393–405.
- David, W.I.F. and Wood, I.G. (1983) Ferroelastic phase transition in BiVO<sub>4</sub>: V. Temperature dependence of Bi<sup>3+</sup> displacement and spontaneous strains. *Journal of Physics*, C16, 5127–5148.
- Dolino, G. (1988) Incommensurate phase transitions in quartz and berillite. In S. Ghose, J.M.D. Coey, and E. Salje, Eds., *Structural and magnetic phase transitions in minerals*. *Advances in Physical Geochemistry*, 7, 17–38.
- (1990) The  $\alpha$ -inc- $\beta$  transitions of quartz: a century of research on displacive phase transitions. *Phase Transitions*, 21, 59–72.
- Dolino, G. and Bachheimer, J.P. (1982) Effect of the  $\alpha$ - $\beta$  transition on mechanical properties of quartz. *Ferroelectrics*, 43, 77–86.
- Dolino, G. and Vallade, M. (1994) Lattice dynamical behavior of anhydrous silica. In *Mineralogical Society of America Reviews in Mineralogy*, 29, 403–431.
- Dolino, G., Bachheimer, J.P., Gervais, F., and Wright, A.F. (1983) La transition  $\alpha - \beta$  du quartz: le point sur quelques problèmes actuels: transition ordre-désordre ou displacive, comportement thermodynamique. *Bulletin de Minéralogie*, 106, 267–285.
- Dolino, G., Bachheimer, J.P., Berge, B., and Zeyen, C.M.E. (1984) Incommensurate phase of quartz: I. Elastic neutron scattering. *Journal de Physique*, 45, 361–371.
- Dolino, G., Berge, B., Vallade, M., and Moussa, F. (1992) Origin of the incommensurate phase of quartz: I. Inelastic neutron scattering study of the high temperature  $\beta$  phase of quartz. *Journal de Physique I*, 2, 1461–1480.
- Dorogokupets, P.I. (1995) Equation of state for lambda transition in quartz. *Journal of Geophysical Research*, 100, 8489–8499.
- Dove, M.T. (1993) *Introduction to lattice dynamics*, 258 p. Cambridge University Press, Cambridge.
- Drebushchak, V.A. and Dement'ev, S.H. (1993) Thermodynamic study of quartz in the vicinity of  $\alpha$ - $\beta$  transition (in Russian). *Geokhimiya*, 1993, 1341–1353.
- Fossum, J.O. (1985) A phenomenological analysis of ultrasound near phase transitions. *Journal of Physics*, C18, 5531–5548.
- Garland, C.W. (1964) Generalised Pippard equations. *Journal of Chemical Physics*, 41, 1005–1008.
- Ghiorso, M.S., Carmichael, I.S.E., and Moret, L.K. (1979) Inverted high-temperature quartz. *Contributions to Mineralogy and Petrology*, 68, 307–323.
- Ginzburg, V.L., Levanyuk, A.P., and Sobyanyin, A.A. (1987) Comments

- on the region of applicability of the Landau theory for structural phase transitions, *Ferroelectrics*, 73, 171–182.
- Grimm, H. and Dorner, B. (1975) On the mechanism of the  $\alpha$ - $\beta$  phase transformation of quartz. *Journal of Physics and Chemistry of Solids*, 36, 407–413.
- Grønqvold, F., Stølen, S., and Svendsen, S.R. (1989) Heat capacity of  $\alpha$  quartz from 298.15 to 847.3 K, and of  $\beta$ -quartz from 847.3 K to 1000 K—transition behaviour and reevaluation of the thermodynamic properties. *Thermochimica Acta*, 139, 225–243.
- Gurevich, V.M. and Khlyustov, V.G. (1979) Calorimeter for determining of low-temperature heat capacity of minerals. Quartz heat capacity under the temperature 9–300 K (in Russian). *Geokhimiya*, 1979, 829–839.
- Heaney, P.J. (1994) Structure and chemistry of the low-pressure silica polymorphs. In *Mineralogical Society of America Reviews in Mineralogy*, 29, 1–40.
- Heaney, P.J. and Veblen, D.R. (1991) Observations of the  $\alpha$ - $\beta$  phase transition in quartz: A review of imaging and diffraction studies and some new results. *American Mineralogist*, 76, 1018–1032.
- Hill, R.J. and Gibbs, G.V. (1979) Variation in  $d(T-O)$ ,  $d(T..T)$ , and  $\angle TOT$  in silica and silicate minerals, phosphates and aluminates. *Acta Crystallographica*, B35, 25–30.
- Höchli, U.T. (1970) Ultrasonic investigation of the first-order  $\alpha$ - $\beta$  phase transition in quartz. *Solid State Communications*, 8, 1487–1490.
- (1972) Elastic constants and soft optical modes in gadolinium molybdate. *Physical Review*, B6, 1814–1823.
- Höchli, U.T. and Scott, J.F. (1971) Displacement parameter, soft-mode frequency, and fluctuations in quartz below its  $\alpha$ - $\beta$  phase transition. *Physical Review Letters*, 26, 1627–1629.
- Hosieni, K.R., Howald, R.A., and Scanlon, M.W. (1985) Thermodynamics of the lambda transition and the equation of state of quartz. *American Mineralogist*, 70, 782–793.
- Hughes, A.J. and Lawson, A.W. (1962) Cylindrical approximation and the  $\alpha$ - $\beta$  quartz transition. *Journal of Chemical Physics*, 36, 2098–2100.
- Kammer, E.W., Pardue, T.E., and Frissel, H.F. (1948) A determination of the elastic constants for beta-quartz. *Journal of Applied Physics*, 19, 265–270.
- Kihara, K. (1990) An X-ray study of the temperature dependence of the quartz structure. *European Journal of Mineralogy*, 2, 63–77.
- (1993) Lattice dynamical calculations of anisotropic temperature factors of atoms in quartz, and the structure of  $\beta$ -quartz. *Physics and Chemistry of Minerals*, 19, 492–501.
- Klement, W., Jr. and Cohen, L.H. (1968) High-low quartz inversion: thermodynamics of the lambda transition. *Journal of Geophysical Research*, 73, 2249–2259.
- Lager, G.A., Jorgensen, J.D., and Rotella, F.J. (1982) Crystal structure and thermal expansion of  $\alpha$ -quartz  $\text{SiO}_2$  at low temperature. *Journal of Applied Physics*, 53, 6751–6756.
- Levanyuk, A.P., Minyukov, S.A., and Vallade, M. (1993) Fluctuation-induced first-order phase transitions near mean-field tricritical points in solids. *Journal of Physics, Condensed Matter*, 5, 4419–4428.
- Lüthi, B. and Rehwald, W. (1981) Ultrasonic studies near structural phase transitions. In K.A. Müller and H. Thomas, Eds., *Structural phase transitions I. Topics in Current Physics*, 23, 131–184. Springer Verlag, Berlin.
- McLellan, A.G. (1973) Thermodynamic stability of the  $\alpha$ - $\beta$  quartz transition. *Philosophical Magazine*, 28, 1077–1086.
- Megaw, H.D. (1973) *Crystal structures: a working approach*, 563 p. Saunders, Philadelphia.
- Mogean, F. (1988) *Propriétés statiques et comportement irréversible de la phase incommensurable du quartz*. Doctoral thesis, Université Joseph Fourier, Grenoble I.
- Nye, J.F. (1985) *Physical properties of crystals*, 329 p. Oxford University Press, Oxford.
- Ohno, I. (1995) Temperature variation of elastic properties of  $\alpha$ -quartz up to the  $\alpha$ - $\beta$  transition. *Journal of Physics of the Earth*, 43, 157–169.
- Pelous, J. and Vacher, R. (1976) Thermal Brillouin scattering in crystalline and fused quartz from 20 to 1000°C. *Solid State Communications*, 18, 657–661.
- Pippard, A.B. (1956) Thermodynamic relations applicable near a lambda-transition. *Philosophical Magazine*, 1, 473–476.
- Pytte, E. (1970) Soft-mode damping and ultrasonic attenuation at a structural phase transition. *Physical Review*, B1, 924–930.
- (1971) Acoustic anomalies at structural phase transitions. In E.J. Samuelsen, E. Anderson, and J. Feder, Eds., *Structural phase transitions and soft modes*. NATO ASI, Norway, 151–169. Scandinavian University Books, Oslo.
- Rehwald, W. (1973) The study of structural phase transitions by means of ultrasonic experiments. *Advances in Physics*, 22, 721–755.
- Richet, P., Bottinga, Y., Denielou, L., Petitet, J.P., and Tequi, C. (1982) Thermodynamic properties of quartz, cristobalite and amorphous  $\text{SiO}_2$ : Drop calorimetry measurements between 1000 and 1800 K and a review from 0 to 2000 K. *Geochimica et Cosmochimica Acta*, 46, 2639–2658.
- Salje, E.K.H. (1988) Structural phase transitions and specific heat anomalies. In NATO ASI Series C, 225, 75–118.
- (1993) *Phase transitions in ferroelastic and co-elastic crystals* (student edition), 229 p. Cambridge University Press, Cambridge.
- Salje, E.K.H., Kuschole, B., Wruck, B., and Kroll, H. (1985) Thermodynamics of sodium feldspar II: experimental results and numerical calculations. *Physics and Chemistry of Minerals*, 12, 99–107.
- Salje, E.K.H., Wruck, B., and Thomas, H. (1991) Order-parameter saturation and low-temperature extension of Landau theory. *Zeitschrift für Physik B*, 82, 399–404.
- Salje, E.K.H., Ridgwell, A., Güttler, B., Wruck, B., Dove, M.T., and Dolino, G. (1992) On the displacive character of the phase transition in quartz: a hard-mode spectroscopic study. *Journal of Physics, Condensed Matter*, 4, 571–577.
- Salje, E.K.H., Graeme-Barber, A., Carpenter, M.A., and Bismayer, U. (1993) Lattice parameters, spontaneous strain and phase transitions in  $\text{Pb}_3(\text{PO}_4)_2$ . *Acta Crystallographica*, B49, 387–392.
- Shapiro, S.M. and Cummins, H.Z. (1968) Critical opalescence in quartz. *Physical Review Letters*, 21, 1578–1582.
- Slonczewski, J.C. and Thomas, H. (1970) Interaction of elastic strain with the structural transition of strontium titanate. *Physical Review*, B1, 3599–3608.
- Smith, G.S. (1963) On the regularity of the tetrahedra in quartz. *Acta Crystallographica*, 16, 542–545.
- Tautz, F.S., Heine, V., Dove, M.T., and Chen, X. (1991) Rigid unit modes in the molecular dynamics simulation of quartz and the incommensurate phase transition. *Physics and Chemistry of Minerals*, 18, 326–336.
- Taylor, D. (1972) The thermal expansion behaviour of the framework silicates. *Mineralogical Magazine*, 38, 593–604.
- Tezuka, Y., Shin, S., and Ishigame, M. (1991) Observation of the silent soft phonon in  $\beta$ -quartz by means of hyper-Raman scattering. *Physical Review Letters*, 18, 2356–2359.
- Toledano, P., Fejer, M.M., and Auld, B.A. (1983) Nonlinear elasticity in proper ferroelastics. *Physical Review*, B27, 5717–5746.
- Unoki, H., Tokumoto, H., and Ishiguro, T. (1984) Brillouin-scattering study of sound velocity of quartz at  $\alpha$ - $\beta$  transition. In W. Eisenmenger, K. Lassmann, and S. Döttinger, Eds., *Phonon scattering in condensed matter* (Springer series in Solid State Sciences, vol. 51), p. 292–294. Springer-Verlag, Heidelberg.
- Vallade, M., Berge, B., and Dolino, G. (1992) Origin of the incommensurate phase of quartz: II. Interpretation of inelastic neutron scattering data. *Journal de Physique I*, 2, 1481–1495.
- Wadhawan, V.K. (1982) *Ferroelasticity and related properties of crystals*. *Phase Transitions*, 3, 3–103.
- Wang, Q., Saunders, G.A., Lambson, E.F., Tschaufeser, P., and Parker, S.C. (1992) Temperature dependence of the acoustic-mode vibrational anharmonicity of quartz from 243 to 393 K. *Physical Review*, B45, 10242–10254.
- Yamamoto, A. (1974) Lattice-dynamical theory of structural phase transition in quartz. *Journal of the Physical Society of Japan*, 37, 797–808.
- Yao, W., Cummins, H.Z., and Bruce, R.H. (1981) Acoustic anomalies

- in terbium molybdate near the improper ferroelastic-ferroelectric phase transition. *Physical Review*, B24, 424–444.
- Young, R.A. (1962) Mechanism of the phase transition in quartz. U.S. Air Force, Office of Scientific Research, Contract no. AF49(638)-624.
- Zubov, V.G. and Firsova, M.M. (1956) The elastic properties of  $\beta$ -quartz at high temperatures. *Soviet Physics, Doklady*, 1, 441–442.
- (1962) Elastic properties of quartz near the  $\alpha$ - $\beta$  transition. *Soviet Physics, Crystallography*, 7, 374–376.

MANUSCRIPT RECEIVED MAY 8, 1997

MANUSCRIPT ACCEPTED SEPTEMBER 12, 1997